UNIVERZITA KOMENSKÉHO V BRATISLAVE
FAKULTA MATEMATIKY, FYZIKY A INFORMATIKY

LIVING WITH LOW VISUAL ACUITY:

AN ANALYSIS OF CORTICAL THICKNESS IN SUBJECTS WITH UNCORRECTED MYOPIA IN THE CONTEXT OF PREDICTIVE PROCESSING

Master's Thesis

2022 Wilma Konrad, BSc

UNIVERZITA KOMENSKÉHO V BRATISLAVE
FAKULTA MATEMATIKY, FYZIKY
A INFORMATIKY

LIVING WITH LOW VISUAL ACUITY:

AN ANALYSIS OF CORTICAL THICKNESS IN SUBJECTS WITH UNCORRECTED MYOPIA IN THE CONTEXT OF PREDICTIVE PROCESSING

Master's Thesis

Study Programme:	Cognitive Science
Field of Study:	Computer Science
Department:	Department of Applied Informatics
Supervisors:	Priv.-Doz. Dr.rer.nat. Natalia Zaretskaya RNDr. Barbora Cimrová, PhD.

2022 Wilma Konrad, BSc

12721564

Univerzita Komenského v Bratislave
Fakulta matematiky, fyziky a informatiky

ZADANIE ZÁVEREČNEJ PRÁCE

Meno a priezvisko študenta: BSc. Wilma Konrad
Študijný program: kognitívna veda (Jednoodborové štúdium, magisterský II. st., denná forma)
Študijný odbor: informatika
Typ záverečnej práce: diplomová
Jazyk záverečnej práce: anglický
Sekundárny jazyk: slovenský

Názov: Living with Low Visual Acuity: An Analysis of Cortical Thickness in Subjects with Uncorrected Myopia in the Context of Predictive Processing
Život s nízkou zrakovou ostrosťou: Analýza hrúbky mozgovej kôry u subjektov s nekorigovanou krátkozrakosťou v kontexte prediktívneho spracovania

Anotácia: V teórii prediktívneho kódovania je percepcia považovaná za aktívny proces neustáleho porovnávania predikcií s prichádzajúcimi senzorickými informáciami. Prípadná nezhoda medzi nimi vedie k upraveniu predikcií na hierarchicky vyšších úrovniach. Predpokladáme, že pri dlhodobej nízkej zrakovej ostrosti dochádza k väčšiemu spoliehaniu sa na predikcie zhora, čo by mohlo viesť k rozdielom v hrúbke zrakovej kôry.

Cieľ: Vykonať experiment s použitím MRI a preskúmať úlohu zrakovej kôry a vzťah medzi zníženou zrakovou ostrosťou a predikčnými procesmi percepcie. Úlohou je preštudovať rozdiely v hrúbke mozgovej kôry u jedincov s nekorigovanou alebo nedostatočne korigovanou krátkozrakosťou v porovnaní so skupinou s ostrým videním alebo plne korigovanou krátkozrakosťou.

Literatúra: Zaretskaya, N. (2021) Zooming-in on higher-level vision: High-resolution fMRI for understanding visual perception and awareness. Prog. Neurobiol., in press, 101998.
Kok, P. & de Lange, F.P. (2015) Predictive Coding in Sensory Cortex. In Forstmann, B.U. & Wagenmakers, E.-J. (eds), An Introduction to Model-Based Cognitive Neuroscience. Springer, New York, pp. 221–244.

Kľúčové slová: procesy zhora-nadol, prediktívne kódovanie, kôrová hrúbka, zraková neostrosť

Vedúci: RNDr. Barbora Cimrová, PhD.
Katedra: FMFI.KAI - Katedra aplikovanej informatiky
Vedúci katedry: prof. Ing. Igor Farkaš, Dr.

Dátum zadania: 31.03.2020

Dátum schválenia: 03.03.2021

prof. Ing. Igor Farkaš, Dr.
garant študijného programu

študent

vedúci práce

12721564

Comenius University in Bratislava
Faculty of Mathematics, Physics and Informatics

THESIS ASSIGNMENT

Name and Surname: BSc. Wilma Konrad
Study programme: Cognitive Science (Single degree study, master II. deg., full time form)
Field of Study: Computer Science
Type of Thesis: Diploma Thesis
Language of Thesis: English
Secondary language: Slovak

Title: Living with Low Visual Acuity: An Analysis of Cortical Thickness in Subjects with Uncorrected Myopia in the Context of Predictive Processing

Annotation: In predictive coding theory perception is assumed to be an active process of constantly matching the expectations with the incoming sensory information. Mismatch between them leads to adjustment of predictions in higher hierarchical levels. We hypothesized that a constant low visual acuity leads to a greater dependence on prediction, which may result in differences of the visual cortex thickness.

Aim: Conduct an MRI experiment to investigate the role of the visual cortex and the relationship between reduced visual acuity and predictive processes in perception. The goal is to examine the differences in cortical thickness in individuals with not optimally- or un-corrected myopia in comparison to a group with fully corrected myopia or emmetropia.

Literature: Zaretskaya, N. (2021) Zooming-in on higher-level vision: High-resolution fMRI for understanding visual perception and awareness. Prog. Neurobiol., in press, 101998.
Kok, P. & de Lange, F.P. (2015) Predictive Coding in Sensory Cortex. In Forstmann, B.U. & Wagenmakers, E.-J. (eds), An Introduction to Model-Based Cognitive Neuroscience. Springer, New York, pp. 221–244.

Keywords: top-down processes, predictive coding, cortical thickness, visual acuity

Supervisor: RNDr. Barbora Cimrová, PhD.
Department: FMFI.KAI - Department of Applied Informatics
Head of department: prof. Ing. Igor Farkaš, Dr.

Assigned: 31.03.2020

Approved: 03.03.2021

prof. Ing. Igor Farkaš, Dr.
Guarantor of Study Programme

Student

Supervisor

Declaration

I hereby declare that I elaborated the presented master's thesis independently using the cited literature.

Acknowledgment

My special thanks go to my supervisors, Priv.-Doz. Dr.rer.nat. Natalia Zaretskaya and RNDr. Barbora Cimrová, PhD., for their patience and their invaluable guidance in the creation of this thesis. Further, I want to thank the Neurovision research team at the University of Graz who worked on the project that served as the basis for this thesis and did not hesitate to help me whenever I had any questions. Also, my brother, who took time off his busy schedule to support me with his advice and expertise. Finally, I would like to thank my family, who encouraged me always and of course to my partner for the various forms of helpful support he has provided throughout the last year.

Abstrakt

ÚVOD: Ľudia s krátkozrakosťou, ktorí odmietajú nosiť optickú korekciu, každodenne zažívajú nízku ostrosť videnia a menej spoľahlivé vizuálne vstupy. Preto sú nútení väčšou mierou sa spoliehať na mozgové procesy, ktoré usmerňujú zrakové vnímanie zhora-nadol (z angl. „top-down processes“). V rámci teórie prediktívneho spracovania to znamená zvýšenú pracovnú záťaž vyšších kôrových oblastí zapojených do generovania predpovedí zhora-nadol a zníženú úlohu nižších vizuálnych oblastí. Bolo ukázané, že hrúbka mozgovej kôry koreluje s kognitívnym zaťažením, a preto môže pomôcť odhadnúť kognitívnu aktivitu v danej oblasti.

Táto štúdia sa zameriava na otázku, či znížená zraková ostrosť u participantov s nekorigovanou krátkozrakosťou súvisí so zmenami v hrúbke mozgovej kôry. V skupine s nekorigovanou krátkozrakosťou sme očakávali zvýšenú hrúbku kôry v parietálnych oblastiach zapojených do vizuálneho spracovania. V prípade okcipitálnej kôry sme neočakávali žiadne rozdiely v dôsledku vzájomného zrušenia zvýšených účinkov zhora-nadol a znížených účinkov zdola-nahor (z angl. „bottom-up“).

METÓDY: 60 účastníkov bolo rozdelených do 3 skupín: prvú tvorili subjekti s nekorigovanou krátkozrakosťou (UM, angl. „uncorrected myopia“), v druhá skupina bola kontrolná skupina s korigovanou krátkozrakosťou (MC, angl. „corrected myopia“) a tretia bola kontrolná skupina s ostrým videním (EC, angl. „emetropic control“). Na meranie hrúbky mozgovej kôry sme využili skenovanie mozgu pomocou magnetickej rezonancie (MRI) a vykonali sme analýzu pre celú mozgovú kôru a pre 13 vopred definovaných oblastí záujmu.

VÝSLEDKY: Oblasť v pravom prednom intraparietálnom záreze sa ukázala byť štatisticky významne hrubšia u UM, v porovnaní s dvoma kontrolnými skupinami. Oblasť v hornej časti pravého parietálneho laloku sa ukázala byť tenšia v MC, v porovnaní s UM a EC. V primárnych zrakových oblastiach okcipitálnej kôry neboli zistené žiadne pozoruhodné rozdiely v hrúbke kôry.

ZÁVER: Naše zistenia naznačujú zvýšenú hrúbku kôry vo vyšších vizuálnych oblastiach u subjektov s nízkou zrakovou ostrosťou. Avšak, v dôsledku malej veľkosti vzorky, štúdia ukazuje nízku štatistickú silu a preto tieto výsledky treba brať s rezervou.

Kľúčové slová:

krátkozrakosť, zrakové vnímanie, prediktívne spracovanie, zhora-nadol, hrúbka kôry, MRI

Abstract

BACKGROUND: People with myopia who refuse to wear optical correction experience low visual acuity and less reliable visual input on an everyday basis. Accordingly, they are required to rely more strongly on top-down processes to guide visual perception. Within the framework of predictive processing theory, this implies increased workload on higher cortical regions involved in the generation of top-down predictions as well as a decreased role of lower visual areas. Cortical thickness has been shown to correlate with cognitive demand and hence can help to estimate cognitive activity in a region.

This study examines whether decreased visual acuity in probands with uncorrected myopia is associated with changes in cortical thickness. We expected increased cortical thickness in the parietal cortex regions involved in visual processing in the uncorrected myopia group. For occipital cortex, we expected no differences due to cancelling out effects of increased top-down and decreased bottom-up effects.

METHODS: 60 participants were divided into 3 groups, one with subjects with uncorrected myopia (UM), one fully corrected myopic control group (MC), and one emmetropic control group (EC). MRI scanning was used to measure cortical thickness and analysis was done for the whole cortex and 13 predefined regions of interest.

RESULTS: One region in the right anterior intraparietal sulcus showed to be significantly thicker in UM than in the two control groups. Also, one region on the right superior parietal lobe showed to be thinner in MC than UM and EC. In primary visual areas of the occipital cortex, no noteworthy differences in cortical thickness were found.

CONCLUSION: The findings revealed clues towards increased thickness in higher visual areas in subjects with low visual acuity, however, the study shows low statistical power due to small sample size.

Keywords:

myopia, visual perception, predictive processing, top-down, cortical thickness, MRI

Content

List of Figures

List of Tables

Abbrevations

aIPS	anterior intraparietal sulcus
EC	emmetropic control
dpt	Diopters
fMRI	functional magnetic resonance imaging
FWHM	full-width half-maximum
GLM	a general linear model
IPS	intraparietal sulcus
KWT	Kruskal-Wallis Test
LGN	lateral geniculate nucleus
LH	left hemisphere
LO1	lateral occipital cortex region I
MAR	minimum angle of resolution
MC	myopic control
MP-RAGE	magnetization-prepared rapid gradient echo
MRI	magnetic resonance imaging
MST	middle superior temporal area
MT	middle temporal area
PP	predictive processing
RH	right hemisphere
ROI	region of interest
SD	standard deviation
SPL	superior parietal lobule
UM	uncorrected myopia
V1	primary visual area
V1d	dorsal portion of primary visual cortex
V1v	ventral portion of primary visual cortex
V2	visual area II
V2d	dorsal portion of visual area II

V2v	ventral portion of visual area II
V3	visual area III
V3d	dorsal portion of visual area III
V3v	ventral portion of visual area III
V4	visual area IV
V5	visual area V
V7	visual area VII
VO1	ventral occipital cortex region I
WRST	Wilcoxon Rank Sum Test

1. Introduction

We live in a world where there is a lot to experience. We evolved to have several channels to sense our environment and be able to interact with it. We perceive this sensory information via sensory receptors which react to inputs from the environment and send electrical signals to the central nervous system.

Neuroscience has managed to understand how receptor cells turn the physical and chemical signals from the environment into electrical nerve impulses. However, there is more to sensation than registration of the physical or chemical energy from the environment and its transduction to the central nervous system. What neuroscience still struggles with is to explain why we perceive identical sets of electrical impulses as being different. How do we make sense of the stimuli we encounter? We also know that our senses are not always 100 percent reliable, our senses can deceive us as it becomes apparent when we look at an optical illusion and see something more than what is physically there. Bistable images nicely illustrate this as they can be perceived in different ways, depending solely on the observer since the physical image does not change (Figure 1) (Rodríguez Martínez & Castillo Parra, 2018).

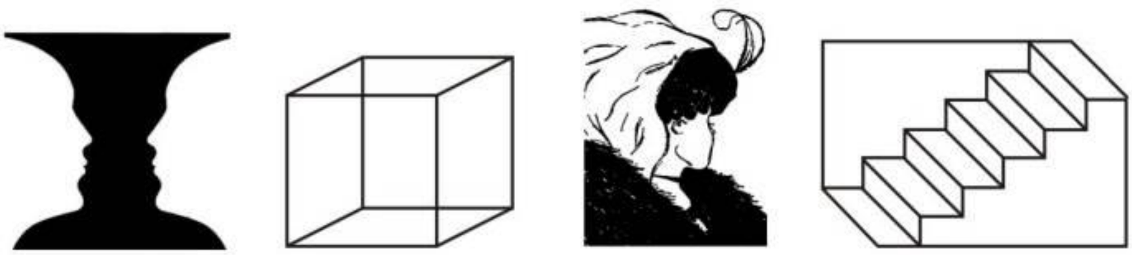

Figure 1: Types of bistable images. From left to right: 1. The vase-face illusion, foreground-background illusion, either two white faces or a black vase is visible; 2. Necker's cube, illusion in perspective; 3. My girlfriend or my mother-in-law, either a young woman or an old woman is visible; 4. The Schröder reversible staircase, illusion in perspective, either regular stairs or upside-down staircase. From (Rodríguez Martínez & Castillo Parra, 2018).

This can be used as a reminder that our sensations are mainly our brains' interpretation of the real world and do not necessarily represent the 'real' world accurately.

For humans, the sensory system we rely most on is the visual sense. This thesis will look at visual perception and the role one specific deficit, namely mild myopia, plays in visual processing. We will consider the findings in the context of perception theories in favor of an internal generative model of perception which refers to the idea that the mind possesses an internal model of the environment that captures the statistical structure of observed inputs as well as tracks the causes that are responsible for the sensory information (Clark, 2013).

In the following chapter, we will discuss visual perception, the anatomical and physiological basics of vision, visual acuity, and myopia as well as the most popular state of the art theories of visual perception.

1.1. Visual Perception

The world around us is filled with information and the nervous system has found mechanisms to access this data in several ways. Our senses help us to see, hear, touch, smell and taste the environment and help to make sense of the surroundings and to create an internal model of the world around us. The interpretations of the sensory input are generated in the nervous system by a series of action potentials passed along the neurons of the sensory pathways (B. Kolb & Whishaw, 2015).

Visual perception is concerned with the perception of light and gives us the sense of sight. How the information about the environment travels through our nervous system will be illustrated in the following section.

1.1.1. The Visual System

The human visual system, like other sensory systems, is organized in a hierarchical manner. It is specialized for the interpretation of a small part of the electromagnetic energy that surrounds us which we call light. The visible spectrum for humans comprises wavelengths of electromagnetic radiation in the range of about 400-700 nm. In this way, it facilitates the visual perception of the environment and the construction of an internal representation of the surroundings (B. Kolb & Whishaw, 2015).

The visual system comprises all the anatomical structures that are involved in visual perception. Starting with the eye and the retina, the information travels along the optic nerve to the optic tract and the lateral geniculate nucleus to the visual cortex (Bear et al., 2020). Figure 2 illustrates the visual pathway in the human brain as displayed in Joukal (2017).

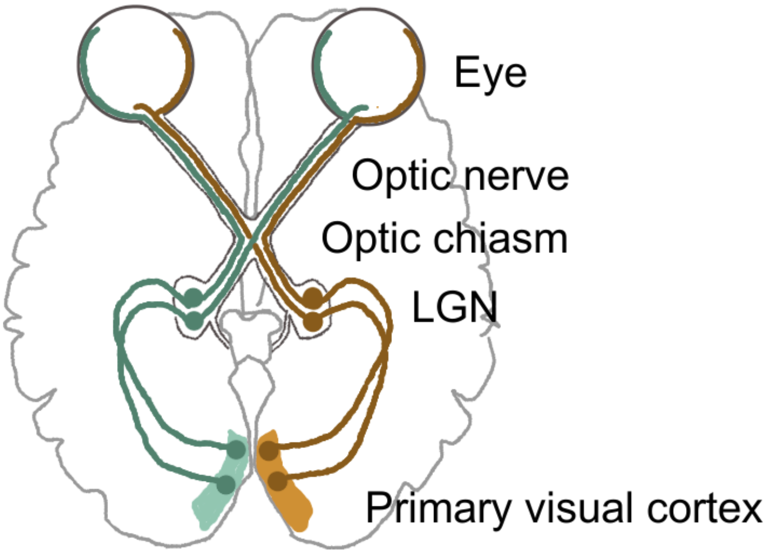

Figure 2: Simplified scheme depicting the visual pathway in the human brain. Adapted from Joukal (2017).

Although the perception of scenes and shapes comes naturally and is effortless for most people, the visual system continuously carries out a number of complex tasks to achieve this experience. Some of these tasks are more ‘basic’ functions like edge detection, motion detection, color vision, and the perception of basic shapes in the visual field. However, the visual system also facilitates more complex tasks like object identification, face recognition, as well as oculomotor coordination in visual search, or visuomotor coordination in object manipulation or locomotion. In addition, since humans possess two eyes, two visual images need to be combined and merged, creating stereopsis which contributes to depth perception.

In the following section, several structures of the human visual system will be introduced individually, and their function will be explained shortly.

1.1.1.1. The Eye

The anatomical structure of the eye bends the incoming light which allows the light to focus on the retina. In the retina the transformation from light energy to neural activity takes place. This is due to the structure of the retina. It contains roughly 125 million photoreceptors of two different types, namely rods and cones which contain light-sensitive photopigments in their membranes. These photopigments lead to a change in membrane potential. Photoreceptors are depolarized in the dark and will hyperpolarize when exposed to light. Rods react sensitively to dim light whereas cones transduce bright light and are used for daytime vision. The human eye has three different types of cones, which enable color vision. Each type of cone is responsive to different wavelengths of light, red, blue, or green (Bear et al., 2020; B. Kolb & Whishaw, 2015).

Each photoreceptor is in synaptic contact with bipolar cells. However, photoreceptors do not fire action potentials, they respond to light changes with graded receptor potentials, meaning a graded change in the membrane potential, resulting in a corresponding change of transmitter release. . Every bipolar cell, in turn, receives input from a cluster of photoreceptors that make up the bipolar cell's receptive field. This receptive field organization is passed from bipolar cells to ganglion cells.

Additionally, there are horizontal cells and amacrine cells that contribute to retinal processing. Horizontal cells receive input from multiple photoreceptor cells and project laterally to influence surrounding bipolar cells and photoreceptors by providing inhibitory feedback. Amacrine cells are also inhibitory interneurons in the retina. They receive their input from bipolar cells and project laterally to surrounding ganglion cells, bipolar cells, and other amacrine cells. They contribute to vertical communication within several retinal layers and are involved in center-surround receptive fields of many ganglion cells as well as the processing of direction-selectivity in the retina (Demb & Singer, 2015)

The output from the retina is the sum of action potentials arising from about 1 million ganglion cells. The ganglion cells' axons form the optic nerve that carries the information to the brain (Bear et al., 2020; B. Kolb & Whishaw, 2015).

1.1.1.2. Retinogenicualte Pathway

The ganglion cell axons form the optic nerve that exits the eye and enters the skull. The optic nerves of both eyes meet to form the optic chiasm where fibres from the nasal retina cross. This ensures that all the information from the left visual hemifield is processed by the right hemisphere and the right visual hemifield is processed by the left hemisphere (Frolov et al., 2017). The part of the ganglion cell axons after the optic chiasm is called the optic tract.

Lesion studies show that the information about the visual world is represented in the retinofugal projection since transections in different sites will lead to different deficits in the visual fields. While damage to the optic nerve will lead to blindness in one eye, harming the optic tract would lead to blindness in one visual hemifield (Frolov et al., 2017).

The information travels via the optic tract to the lateral geniculate nucleus (LGN) of the dorsal thalamus, which is the major target of the retinal ganglion cells. However, a small set of fibers from the optic nerve projects to other structures like the hypothalamus and the midbrain. The hypothalamus is concerned with hormone regulation and controls a variety of biological rhythms (Li & Li, 2018). The midbrain is involved in eye movement and control of the size of the pupil. The superior colliculus in particular is connected to motor neurons in the brain stem and can trigger eye and head movements (Bear et al., 2020).

1.1.1.3. The Lateral Geniculate Nucleus

The LGN neurons receive synaptic input from the retinal ganglion cells and project axons to the primary visual cortex (Bear et al., 2020). The right and the left LGN are arranged in six distinct layers of cells that are bent around the optic tract. Different layers in the LGN receive input from different ganglion cells and ganglion cell types and their receptive fields. Since the axons of the nasal retina cross in the optic chiasm, each LGN receives information from both, the ipsilateral and the contralateral eye. These fibers synapse with different layers in the LGN so the information from each eye is stored in adjacent layers of the LGN (Kerschensteiner

& Guido, 2017; B. Kolb & Whishaw, 2015). Furthermore, the retinal topography of the visual field is reproduced in the LGN (Bear et al., 2020; B. Kolb & Whishaw, 2015).

To achieve a unified visual impression despite two eyes and two slightly different visual perspectives, the brain needs to combine these two distinct inputs. The information from one eye needs to be combined with information from the other eye (Dougherty et al., 2019). Recent studies in mouse LGN suggest that binocularity, as well as the binocular rivalry, may be related to the LGN (in addition to the primary visual cortex). In addition to strictly monocular neurons, trans-synaptic tracing studies found thalamocortical neurons that receive input from both eyes (Dougherty et al., 2019).

Overall, only a small percentage of the incoming information comes from the retina, the vast majority of inputs into the LGN comes from other neuronal structures like the brainstem, cholinergic nuclei, and the thalamic reticular nucleus (Kerschensteiner & Guido, 2017; J. L. Morgan, 2017). By far the strongest input comes from the feedback projections from the primary visual cortex. In rodent studies, the percentage of nonretinal inputs made up to 90% (Kerschensteiner & Guido, 2017; Rose & Bonhoeffer, 2018). In human LGN the percentage of synaptic input from the primary visual cortex is estimated to be around 80% (Bear et al., 2020).

The LGN in turn gives rise to the optic radiation. The optic radiation consists of axons that project to the primary visual cortex.

1.1.1.4. Primary Visual Cortex

1.1.1.4.1. Anatomical Aspects

Most of the LGN neurons form synapses with cells of the primary visual cortex (V1). The primary visual cortex is also called Brodmann's area 17 or striate cortex and is located in the occipital lobe. Anatomically, the primary visual cortex stretches rostrally almost to the lunate sulcus and on the posterior-lateral side the inferior occipital sulcus where it forms the border to the visual cortex area II (V2) (Bear et al., 2020; Schmolesky, 1995).

1.1.1.4.2. Cell Types

The primary visual cortex is composed of neurons in different shapes, most of which fall under the category of either spiny stellate cells, pyramidal cells, or interneurons (Bear et al., 2020; Schmolesky, 1995). Spiny stellate cells are excitatory and generally smaller with spine-covered dendrites and predominately occur in cortical layer four (Bear et al., 2020). Pyramidal cells are also excitatory cells, their cell body is shaped like a pyramid and is characterized by a single thick dendrite that branches and extends toward the white matter as well as basal dendrites that extend horizontally (Bear et al., 2020). Finally, interneurons are GABAergic cells that play a critical role in inhibition (Kepecs & Fishell, 2014) Interneurons compose approximately 20% of the neurons in the cortical layers 2-6 (Schmolesky, 1995).

1.1.1.4.3. Functional Organization

In V1 retinotopy is preserved, hence neighboring neurons in the retina feed information to neighboring neurons in the V1 in order to preserve the visual field (Bear et al., 2020). Like all primary sensory cortex regions, the primate primary visual cortex can be organized in laminar and columnar fashion (Hubel & Wiesel, 1972). Cortical organizations in columns refers to cell clusters that are vertically arranged and form column-like structures from the surface of the cortex to the white matter. They can be defined by anatomical features and/or functional features like ocular dominance or color vision (Hubel & Wiesel, 1972; Schmolesky, 1995).

1.1.1.4.4. Cortical Layers

When considering the laminar organization, V1 consists of six layers as introduced by Brodmann, with layer I being the most superficial layer and layer VI the deepest layer. Most of the layers show sublayers resulting in at least 12 sublayers. Overall, V1 layers can be roughly subdivided into superficial (layers I-III), middle (layer IV), and deep (layers V and VI).

The most superficial layer I is mostly composed of dendritic and axonal synapses formed by pyramidal cells in the cortex, the input from LGN, the pulvinar, and feedback connections from other cortical areas and subcortical regions. The supragranular layers II and IIIA contain many axons and dendrites of neurons from other cortical layers and receive some thalamic input but no direct input from the middle layer IVC. Layer IIIB in turn has very strong input from the middle layer IVC.

The middle layer IV is divided into three sublayers. Layer IVA does not contain pyramidal cells which sets it apart from layer IIIB. Layer IVB has some pyramidal cells in a very low density but receives strong input from IVC. IVB has connections with V2 and other higher visual cortex areas, providing information for the dorsal processing stream. Layer IVC shows a high density of stellate cells. Based on histology, innervation patterns, and physiological properties layer IVC was further divided into IVCα and IVCβ (Blasdel & Fitzpatrick, 1984). IVCα projects heavily to IVB. IVCβ shows dense innervation of IVA and IIIB, as well as some innervation in IVC, V, and VI (Hubel & Wiesel, 1972; Schmolesky, 1995).

In layer VA, most neurons seem to project to layer IIIB and layer I. In VB sends axons to layer IIIA (Lund et al., 1977). Layer VI sends recurrent axons to layer IV. Other neurons in this layer form a neural loop with the LGN by projecting axons to LGN and receiving input from there (Schmolesky, 1995).

Although a lot is known about the anatomy and the connections of the cortical layers, the exact function of each layer has not been investigated properly yet (Adesnik & Naka, 2018).

1.1.1.4.5. Connectivity of the Primary Visual Cortex

The inputs and outputs of the primary visual cortex are distributed across different layers. Input signals from LGN enter the V1 cortex through a subset of cortical layers, with the largest portion of fibers terminating in layer IV.

There are intracortical connections most of which run radially from the white matter to the superficial layer I. These radial intracortical connections help to maintain retinotopy. There are also horizontal connections between cells in certain layers of the visual cortex. These connections play different roles in the analysis of the visual input.

Concerning the output of V1, pyramidal cells in different layers innervate different structures. Whereas the ‘supragranular’ layers II, III, and parts of layer IV innervate different cortical areas, the ‘infragranular’ layer V forms connections with the pons and superior colliculus in the midbrain, and layer VI cells form massive projections back to the LGN (Bear et al., 2020).

1.1.1.4.6. Physiology

Hubel and Wiesel were the first ones to systematically describe V1 physiology. They found neurons in the primary visual cortex that are responsible for an array of visual functions like color, orientation selectivity, direction selectivity, and binocularity (Hubel & Wiesel, 1962).

The central concept for describing V1 physiology is the receptive field. ‘Receptive field’ refers to a discrete area relative to the fovea where the presentation (or removal) of a stimulus will cause activity in the neuron associated with this specific receptive field. Stimuli outside the receptive field will not alter the activity of the associated neuron (Schmolesky, 1995).

Different receptive field properties are distributed differently across the cortical layers. For example, receptive fields sensitive to the wavelength of light with center-surround opponency can be found primarily in layer IVCβ (Bear et al., 2020; Garg et al., 2019). Binocular receptive fields respond to visual input from either eye in both hemispheres of the V1 where retinotopy is preserved. This is crucial for binocular animals and these receptive fields lay the foundation for binocular vision. These receptive fields are primarily found in the more superficial layers prior to IVC (Bear et al., 2020; Hubel & Wiesel, 1962). As for orientation- and direction-selective receptive fields, Hubel and Wiesel (1962) found that many neurons in V1 respond to a bar of light in a particular orientation moving across their receptive field particularly well. They found that most neurons outside IVC and some even inside IVC exhibit orientation selectivity. Orientation selectivity is crucial for the analysis of an object's shape. Many orientation-sensitive receptive fields in V1 also show direction sensitivity. Such neurons respond when a bar of their optimal orientation moves in the direction that is orthogonal to the orientation. This is the basis for the perception of motion (Bear et al., 2020).

1.1.1.5. Visual Areas 2 and 3

Visual area II (V2) is also referred to as Brodmann’s area 18. It is present in both hemispheres and surrounds V1 (Sereno et al., 1995). V2 receives input from V1 as well as significant thalamic input from the pulvinar (Dumoulin et al., 2017). Like the primary visual cortex, V2 contains cells that are sensitive to orientation, color, and spatial frequency. Additionally, cells in V2 show activity to combinations of orientations and more complex patterns (Anzai et al., 2007). Furthermore, figure-background organization and sensitivity for binocular disparity enable gestalt organization of the perceptual input (Qiu & von der Heydt, 2005).

There is some debate about the location, spatial extent, role, and even existence of visual area III (V3) across primates (Kaas & Lyon, 2001). V3 has been found to share continuous foveal confluence with V2 (Schira et al., 2009). V3 has been found to play a role in object recognition (Ayzenberg et al., 2022) as well as motion perception (Braddick et al., 2001).

1.1.1.6. Association Cortex

Visual processing beyond the early processing regions V1, V2, and V3 is frequently separated into two cortical streams. The ‘dorsal stream’ and the ‘ventral stream’ have been studied in the monkey cortex (Bear et al., 2020). The division of cortical visual areas into these two ‘streams’ was due to different behavioral responses to stimuli and different connectivity (Milner, 2017).

The ‘ventral stream’ of visual processing includes visual area IV (V4) and the inferior parts of the temporal lobe. This stream is thought to be involved to object recognition and perception of the visual world (Bear et al., 2020; Milner, 2017). In experiments on primates, V4 played a role in color and shape perception. Lesions to this region resulted in specific perceptual deficits rather than visual field blindness as is the case in the early processing regions (Winawer & Witthoft, 2015). The inferior temporal lobe is involved in visual perception and visual memory as well in the perception of faces in particular (Bear et al., 2020). Areas of the ventral stream project to structures in the temporal and frontal lobes that are involved in memory, emotion, and social behavior (Milner, 2017).

The ‘dorsal stream’ on the other hand stretches dorsally from V1 toward the parietal lobe. This processing stream is known to involve the visual area 5 (V5)/middle temporal (MT) area and the medial superior temporal (MST) area. The dorsal stream is generally considered to be involved in the visual processing of motion and the visual control of action. Neurons in the MT region are particularly direction-sensitive and respond to motion (Bear et al., 2020). The intraparietal sulcus (IPS) is generally assumed to be part of the dorsal stream. IPS responds to tasks that are related to visual attention and the direction of eye movements, as well as the encoding of multimodal motion and tasks like reaching and grasping. Several regions in the IPS can be distinguished based on several functional as well as structural criteria (Konen & Kastner, 2008). Direct pathways exist from the occipito-parietal dorsal stream to subcortical structures like the superior colliculus and brain structures that are involved in eye movement and parts of the spinal cord that controls the limbs (Milner, 2017). In the ventral stream, these connections are not present or not to that extend.

There is evidence that these two streams are not completely separate but interact. Systems that are associated with the ventral stream have been found to mediate complex visuomotor skills, and systems that are associated with the dorsal stream have been found to part in certain aspects of the 3D perceptual function of the ventral stream (Milner, 2017).

Furthermore, there is evidence that this list is not exhausted and there might be additional processing streams in the human brain for different facets of visual perception (Pitcher & Ungerleider, 2021).

1.1.2. Visual Acuity

Visual acuity refers to the measure of clearness of vision. It is an important measure in the attempt to quantify the subjective visual impression of an individual. There are different kinds of visual acuity measures that are concerned with different aspects of visual perception. Here we focus on visual acuity that refers to the clearness of vision defined as the individual’s ability to recognize small details (Heinrich & Hoffmann, 2018).

Although most people might have an intuitive understanding of the term, it is important to keep in mind that visual acuity is operationally defined and is the measure that results from a standardized procedure that is designed to ensure comparability (Heinrich & Hoffmann, 2018). This procedure is normally a vision test, performed by an eye-care professional. This measure indicates how well small details are resolved in the very center of the visual field, the fovea centralis.

In order to quantify visual acuity, in 1861 the ophthalmologist Donders defined visual acuity as the difference between a subject's performance and standard performance. This standard performance or normal visual acuity was later defined by the ophthalmologist Herman Snellen as the resolution of the eye which makes it possible to separate contours that are 1 arc minute apart (Colenbrandner, 1989).

In practice, the visual acuity test is performed by an examinee and an examiner. The examiner presents optotypes with decreasing size to the person undergoing the examination. Optotypes are visual symbols like stylized letters, Landolt rings, pictures, or symbols for children or the illiterate that are viewed from a predefined viewing distance. To maximize the contrast, the optotypes are represented as black symbols against a white background (Kniestedt & Stamper, 2003). Far acuity is measured in a vision test that shows the optotypes at 6 meters distance. This distance is considered to be optical 'infinity', i.e., a distance at which the eye is relaxed and does not need to accommodate. Near acuity is usually concerned with the identification of optotypes at reading distance, at about 0,30 meters.

The visual acuity depends on the size of the smallest optotype recognizable. It can be expressed as a fraction where:

$$\text{Visual Acuity} = \frac{\text{Optimal viewing distance}}{\text{Actual viewing distance}}$$

For normal vision, this would mean that an optotype that is designed to be legible from 6 meters distance can be recognized from the actual 6 m distance.

$$\text{Normal visual acuity} = \frac{6}{6} = 1.0$$

The visual acuity is quantified by measuring the smallest distance at which two contours appear to be separated.

Most optotypes are designed to have a critical gap, a gap in the contour of the optotype that is essential for discrimination (e.g., Landolt C). The identification of the critical gap in the optotype thus allows measuring the visual acuity. The critical gap typically amounts to 1/5th of the size of the optotype, hence visual acuity is determined by the size of the optotype and the distance at which it is viewed. The size of optotypes is determined by the angle under which the optotype subtends at the eye which is measured in arc minutes. The reciprocal value of the size of the critical gap in the smallest optotype recognizable is used to determine the visual acuity. Visual acuity can be expressed as simple fractions or as decimals. Furthermore, a LogMAR scale can be used that quantifies visual acuity as the decadic logarithm of the minimum angle of resolution (MAR) (Gräf, 2012).

Visual acuity can be influenced by a number of factors that can affect any part of the visual system. Neural factors concern the sensitivity and the functioning of the brain regions involved in visual perception. The clearness and the refractive power of the structures and media of the external eye, and most importantly, the physiological functioning and integrity of the retina and the optical nerve have a severe impact on the subjective visual perception and visual acuity.

1.1.3. Myopia

Myopia is colloquially known as near-sightedness and is a refractive error of the eye where the focus of the light entering the eye lies not directly on the retina. Due to a disbalance of the refractive power of the lens and the axial length of the eye, the resulting light focus in myopic eyes lies in front of the retina (Baird et al., 2020). Depending on the severity of myopia, the visual far point of the eye is closer than it is in emmetropic eyes, resulting in a blurred image when looking at objects beyond that distance. The visual far point can be described as the farthest point from the eye that is still focussed on the retina and therefore perceived as clear. In unaccommodated emmetropic eyes, this point is at infinity. However, in medical practice, it is assumed to be 6 meters because the accommodation change from 6 meters to infinity is negligible.

The magnitude of myopia is measured in diopters (dpt). Diopters are the unit of measurement of the power of an optical lens, and it is equal to the reciprocal focal length. The magnitude measured in myopic eyes refers to the power of the lens that corrects myopia to ideal visual acuity. The lenses that are used to correct myopic ametropia are concave lenses that diverge the light beams in order to focus on the retina. As for this characteristic, concave lenses are denoted with a negative value. The higher the negative diopter value the stronger the power of the concave lens (Spraul & Lang, 2008).

The diagnosis is normally made by an eye care professional. Myopia is defined at a spherical equivalent of -0,5 dpt or more. Typically, -6 dpt or more are referred to as ‘high myopia’. Higher degree myopia can be a risk factor for multiple other ocular disorders (Baird et al., 2020). Up to this point, there are no universally accepted approaches to obviate the emergence of myopia. The most common treatment for myopia is optical correction with concave lenses in the form of glasses or contact lenses. The shape of the lens allows bending the light entering the eye which focuses the image accurately on the retina, thus creating a clear image (Cooper & Tkatchenko, 2018). Another less common way to treat myopia is with refractive surgery (Gomel et al., 2018). Furthermore, myopia can be combined with other refractive errors like astigmatism or presbyopia.

Myopia is a very widespread disorder affecting about 28.3% of the global population. About 4.0% of the global population is diagnosed with high myopia (Holden et al., 2016). The prevalence of early-onset myopia that tends to first occur before the age of 11 is increasing. Early-onset myopia leaves more time for myopia to increase until the mid-twenties when refraction stabilizes, typically leading to higher degrees of myopia. This suggests an increase in the prevalence of myopia and high-degree myopia in the next few decades. According to estimates, 49.9% of the world population will be affected by short-sightedness by the year 2050 (Baird et al., 2020; Holden et al., 2016).

The exact cause for myopia is not yet known but it is believed to be a combination of environmental and genetic factors. Risk factors for the development of myopia include a family history of the condition and continuous near work. The recent rise in affected individuals in the past few decades suggests a strong influence of environmental factors as the genetic predisposition has not substantially changed. Such environmental factors comprise and a higher number of years in education and increased near-work activities, like for example the use of computers, electronic mobile devices, and books. Moreover, recent studies found a possible connection between the development of myopia (as well as its degree) and less time spent outdoors, which is thought to be connected with exposure to daylight (I. G. Morgan et al., 2021).

Some locations in East and Southeast Asia show a strikingly high prevalence of myopia (47.0%) when compared to Central Europe (27.1%), Central Asia (17.0%), and Central Africa (7.0%). Myopia is particularly frequent in urbanized areas (Baird et al., 2020).

1.2. Cortical Thickness

The neocortex is a tightly folded sheet of neurons that forms the outer layer of the cerebrum and can be as large as 2500 square centimeters. Its thickness varies from 1.5mm to 4.5 mm (Jiang et al., 2016; B. Kolb & Whishaw, 2015). The thickness of the neocortex can reflect the size, density, and arrangement of neurons in the cortex which is closely linked to cognitive ability (Narr et al., 2007).

The neocortex shows a high degree of neuroplasticity. Neuroplasticity refers to the ability of the nervous system to alter synaptic connections in order to adapt their function and structure in response to experience, for example, environmental changes and injuries (Baroncelli & Lunghi, 2021).

In longitudinal studies, cortical thickness in most areas declined linearly with age over time with the main effect present in the oldest part of the sample. This is not limited to cortical thickness in subjects with neurodegenerative disorders like dementia, but can also be found in physiological healthy aging (Fjell et al., 2014; Thambisetty et al., 2010). Healthy aging involves changes in the brain that are often accompanied by changes in cognitive and motor functions. These changes can result in gradual impairment of activities of daily living. However, the exact cause for this physiological decline is not clear yet. (Burnett-Zeigler et al., 2012).

Recent studies show, that not only neuroplasticity is still present in adult brains, but to a much higher degree than previously assumed. (Castaldi et al., 2020). Yet, also in the ability for neuroplastic mechanisms seems to undergo a decline during a lifetime. Again, the reason for these age-associated changes in plasticity is not worked out yet, however, environmental, and biological factors like diet, physical activity, chronic stress, sleep deprivation, etc. are discussed to play a role in these processes (Freitas et al., 2011).

Anyhow, the cortex is not solely subject to decline. In experiments, the neocortex has been shown to change in response to cognitive stimulation. Engvig and collaborators (2010) examined cortical thickness after memory training in elderly subjects. They found an increase in thickness in cortex regions associated with memory training. Additionally, they found that the thickness of these areas correlated positively with the success of the training.

For the visual cortex, in particular, recent studies suggest even short-term interventions like monocular or binocular deprivations in adult subjects lead to homeostatic changes in the visual cortex. These chemical changes can facilitate structural changes when maintained for an extended period of time (Castaldi et al., 2020).

The thickness in the primary visual cortex has been shown to decrease in response to central vision loss caused by age-related macular degeneration (Burge et al., 2016).

These studies point towards the fact that the thickness in cortical regions correlates with the cognitive demand on these regions. Cognitive stimulation and increased cognitive demand when maintained over some time, alter the structural properties of the cortex like the size and the density of neurons, leading to an increase in cortical thickness. Hence, the thickness serves as an important marker for multiple aspects of brain functioning and measurements of cortical thickness can provide important information about the regional integrity of the cerebral cortex as well as cognitive demand on these regions (Jiang et al., 2016).

1.3. Theories of Visual Perception

The process of how the central nervous system accesses visual information and how the visual system works has been discussed in the previous sections. However, how exactly the mind extracts visual information from the environment so efficiently as it does cannot be answered satisfactorily with this information alone. Visual perception is a complex process that has received quite some attention in the past decades. Many psychologists, philosophers, and neuroscientists have attempted to answer this question and came up with different theories on how the mind perceives. Some of the main theories and movements that have dominated psychological research in the 20th century will be mentioned now in the following section.

To begin with, there is the theory of direct perception, which proposes that perception equals the unmediated detection of bottom-up information from the environment. According to this theory, sensory stimulation alone carries all the information that is necessary in order to perceive the environment (Kubovy et al., 2013).

The view of direct perception can be contrasted with the theory of cognitive constructivism. The main notion of cognitive constructivism is that visual perception is made possible by inductive inference. Perception works beyond one's awareness and combines visual input with general and context-specific knowledge. The mechanisms and cognitive operations for perception are the same as for conscious inference and problem-solving. Cognitive constructivism is famously associated with Helmholtz's doctrine of unconscious inference (Helmholtz, 2005). This theory implies that human vision is incomplete and the unconscious mind infers a complete picture like for example, motion and depth perception.

In the early decades of the 20th century, another school in psychology emerged that was concerned with the perceptual process, namely Gestalt theory. Well-known representatives of this movement are Wertheimer, Kohler, and Koffka (Kubovy et al., 2013). This approach states that the brain as a dynamical system automatically parses and organizes the perceptual world into shapes and patterns. The resulting Gestalt may have emergent properties that the single component lacks. As a dynamical system that instantiates self-organizing processes, Gestalt theory rejects the idea of centralized top-down regulation of perception (Kubovy et al., 2013; Wagemans et al., 2012).

1.3.1. Predictive Processing Theory

The theory of predictive processing (PP) follows Helmholtz's idea of perception as an active inference rather than a passive observation of the environment (Clark, 2013). PP originates in information technology. In order to increase speed and efficiency when working with a high amount of data, only changes in the data are processed.

In PP theory the brain has an internal concept of the environment, a generative model which is based on prior experience.

The generative model continuously tracks the entire scene and the causal matrix that is responsible for the visual input that is perceived at this very moment. Based on experience and the likelihood at this given moment, the mind tries to predict the flow of incoming sensory data. These inferences are based on prior experience as good guesses are used to increase the posterior probability of the internal model. The causal matrix contains possible causes and explanations for the sensory input, for example in visual perception the generative model accounts for a temporal element that makes the processing of object trajectories possible (Clark, 2013). At the core of PP theory lies the assumption that the brain is hierarchically structured.

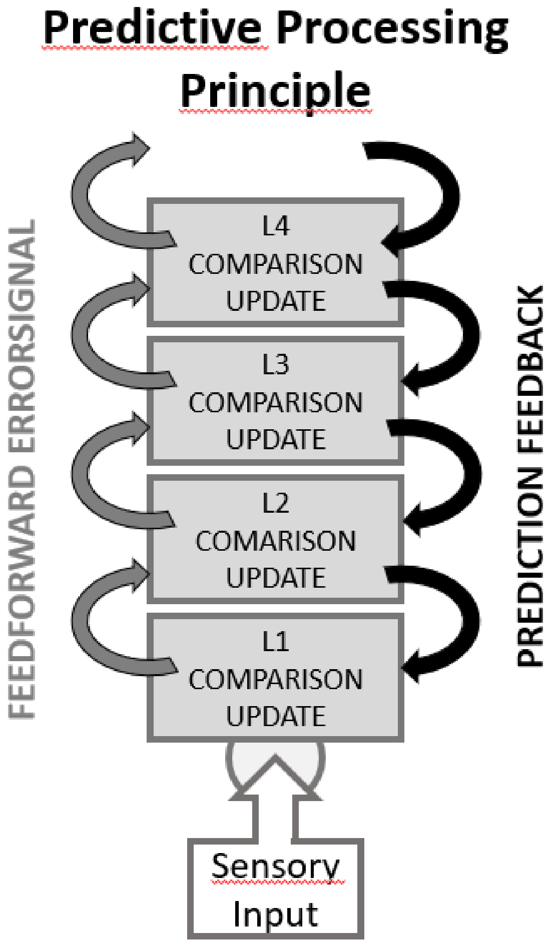

Figure 3: Basic principle of prediction updating in PP theory in the hierarchical layers (L1-L4). Sensory input gets compared to top-down prediction in L1. This generates an error signal that is used to update the prediction in L2 which in turn generates an error signal etc. Eventually the error signal will be used to update the generative model.

At each hierarchical level, the actual bottom-up sensory input is compared to the top-down predictions that are thought to descend the hierarchy. At each hierarchical layer, the prediction errors are calculated and used to alter the prediction in the higher hierarchical layer and ultimately update the internal generative model.

The current best model is then used as a prior in the lower hierarchical level, engaging in a process of iterative estimation. This allows priors as well as models to co-evolve across multiple linked layers of processing in order to account for the sensory data (Figure 3). According to PP, what the mind actually perceives are the deviations in the expected input.

Prediction signals continuously descend the hierarchy while error signals ascend the hierarchy. This is performed in an iterative manner. According to Clark (2013), this leads to a minimization of the prediction error at each level in order to optimize and enhance the accuracy of perception and recognition and thereby minimizing free energy.

Free energy in this context refers to Karl Friston's free energy principle (Friston, 2010). According to this theory, thermodynamic free energy refers to the energy available to do useful work. When applied to the cognitive domain it can be interpreted as the difference between how the world appears to be and the way it actually is. The better the fit, the lower the free energy.

The prediction error, which arises when the predicted input doesn't match the actual input can be equated with 'surprisal' for the mind. In this context, entropy is the long-term average of surprisal. Therefore, reducing free energy reduces surprise and entropy. This means good predictions help avoid harm to the individual in their exchange with the environment (Friston, 2010).

1.3.1.1. Evidence for Predictive Processing

Predictive processing is supported by two main sources of evidence. Indirect support for PP can be found in computational modeling of PP strategies for the simulation of observed behavior in humans and mammals (Clark, 2013). As for evidence in living organisms, examples of predictive coding have been identified in multiple instances involving hearing (Sohoglu & Chait, 2016), touch (Peyrache et al., 2015), the representation of space in the hippocampus (Stachenfeld et al., 2017) and vision (Hosoya et al., 2005; Johnston et al., 2019).

1.3.1.1.1. Bayesian Evidence

PP proposes that the brain is constantly dealing with a varying degree of uncertainty and makes use of Bayesian inference in order to interact with an uncertain environment.

The Bayesian approach to perception assumes a conditional probability density function for sensory information which is applied over a set of unknown variables i.e., a posterior density function.

For example, a Bayesian perceptual system would represent a perceived component (e.g., depth of an object) not as a single value but as a conditional probability density function (e.g., p(Z/I)). This would specify the relative probability that the object is at a different depth (Z), given the available sensory information (I).

Meaning, the underlying component computations that are the basis of Bayesian inferences are performed on the representations of conditional probability density functions rather than on unitary estimates of parameter values.

For each parameter computed, an optimal Bayes' system maintains a representation of all possible values along with their probabilities. This allows the system to function efficiently over space and time and to integrate different sensory modalities. Considering predictive coding, this further allows the brain to propagate the information from one level of processing to another without having to commit to a particular interpretation (Knill & Pouget, 2004).

Good predictions increase the posterior probability of the current model of the environment and are propagated down the hierarchical structure where they serve as a source of the prior in the level below.

PP assumes a bidirectional hierarchical structure that creates 'empirical priors': one level passes constraints on to the lower levels in the hierarchy where these constraints are progressively tuned by the sensory input itself (Clark, 2013).

There is some evidence for this in psychological experiments on cue integration that would support PP theory in sensory processing. In these experiments, human subjects show the ability to optimally weigh various cues through distinct sensory modalities in a way that reflects the current levels of uncertainty (Ernst & Banks, 2002; Knill & Pouget, 2004). Another good example for PP is the Bayesian understanding of color perception which accounts for well-known phenomena like color constancy and some optical illusions (Brainard, 2009). There are also attempts to explain phenomena like binocular rivalry with PP theory (Clark, 2013).

Evidence for predictive processing can be observed at multiple processing stages on the neural level. For example, it is known that retinal ganglion cells take part in some sort of predictive coding, insofar as the receptive fields show center-surround antagonism. In other words, what is conveyed is the departure from the predictable structure if the center of the receptive field differs from the expected surroundings (Hosoya et al., 2005). However, some retinal ganglion cells have been observed to alter their sensitivity to orientation in becoming less sensitive to common orientations in the input as opposed to uncommon orientations (Gollisch & Meister, 2010; Hosoya et al., 2005).

1.3.1.1.2. Evidence for Predictive Processing in Early Visual Cortex

The primary visual cortex V1 is involved in the grouping of edges and lines into coherent shapes. PP theory states that that feedback connections carry predictions while feedforward connections signal the prediction errors between top-down predictions and bottom-up sensory input (Figure 3). Within this framework, the effect of feedback on V1 may be either enhancing or suppressive, depending on whether the prediction is good, and the feedback signal is met by congruent bottom-up input.

Kok and de Lange (2014) tried to quantify the spatial profile of neural activity in the early visual cortex during shape perception and found that neural activity increases in regions of V1 that have receptive fields on the shape but lack bottom-up input. Neural activity in regions that receive bottom-up sensory input that is predicted by the shape was found to be suppressed during shape perception. This suggests that shape perception changes lower-order sensory representations in a highly specific and automatic manner, in line with PP theories (Kok & de Lange, 2014).

Some experiments have been performed to investigate the role of surprise in the brain. Summerfield and colleagues (2008) showed in their fMRI study that when stimulus repetitions were likely and were already anticipated, the stimuli led to a strongly reduced neural response. Due to the method used in this experiment, it was not possible to investigate whether predictability had a suppressive effect on the (predicted) sensory input or whether surprising events alter the direction of visual attention. Consecutive experiments indicated rather a suppression effect of prediction on the sensory input and that prediction suppression effects are independent of those of bottom-up adaption (Todorovic et al., 2011; Todorovic & de Lange, 2012).

Other studies investigated the encoding of prediction in higher-level sensory tasks like apparent motion where static stimuli induce the illusion of motion. In these experiments, the areas of the primary visual cortex (V1) which normally correspond retinotopically to visual stimulation along the trajectory of illusory motion, have shown activity during the perception of illusory motion (Muckli et al., 2005). According to Kok (2015), this could be due to higher-level motion-sensitive areas, like MT/V5, assuming motion in the static images and signaling predictions of the ‘moving’ stimuli back to V1.

In a predictive coding framework, prediction plays a strong role. In order for predictions to alter hypotheses on perceptual content, prior expectations on the sensory input may be hypothesized to be activated prior to the sensory stimulus (Kok, 2015). This was confirmed in studies that examined activity in the sensory cortex when a predicted stimulus was not present in the bottom-up sensory input (den Ouden et al., 2009).

Kok and de Lange (2014) showed participants different pairs of auditory cues paired with visual cues and measured neural activity in V1. After the participants had learned the pairs, only the auditory signal was presented, and the associated visual signal was omitted. They found that in these trials, the activity pattern in V1 was similar to the trials where the visual and the auditory stimulus were present. Hence, the activity in the primary visual cortex was triggered by the expectation (or prediction) of the paired visual stimulus. They further found that the expectation even carried information about the associated visual stimulus that was expected to appear. In experiments on macaques the presence of prediction, in the form of an activity that appeared prior to the sensory input and which was specific to the representation it anticipated was confirmed (Meyer & Olson, 2011). This is evidence that the observed activity is related to predictions rather than prediction errors caused by the lack of expected visual input.

In their fMRI study, Murray and collaborators examined activity in V1 during shape perception. They showed participants visual elements that could be either perceived as random elements or as elements that could be grouped into coherent shapes. During the trails with grouped elements, they observed increased activity in higher visual areas involved in shape perception and decreased visual acuity in V1. This is consistent with predictive coding theories where higher visual areas ‘explain away’ the incoming visual information (Murray et al., 2002).

Attention has served as an alternative explanation for the neural activity attributed to prediction generation in the predictive coding framework. However, attention itself can be explained with predictive coding and does not necessarily contradict it (Kok, 2015). In interaction with a stochastic environment, a wide array of sensory inputs with a varying degree of noise is processed simultaneously. Hence, some of the incoming signals are more reliable than others. Within the predictive coding framework, to navigate efficiently the precision of the sensory inputs and prediction errors becomes relevant. Where less noisy signals should be used to update the current hypotheses, noisier signals should be identified as less reliable, thus being weighed less. Accordingly, bottom-up perception should be driven by sensory input with high precision, whereas low precision in sensory signals requires a stronger role of top-down inferences (Kok, 2015).

Attention could be the process through which the brain modulates its precision estimates of the incoming signal (Feldman & Friston, 2010). By increasing the precision of certain prediction errors, attention increases its weight in perceptual inference (Kok, 2015). Thus, prediction is directed in a ‘top-down’ manner to enable the processing of visual information whereas attention is processed ‘bottom-up’ since it is attracted by salient stimuli from the outside. However, the behavioral effects of attention and prediction seem to be superficially identical (Summerfield & Egner, 2009).

Although some models of predictive coding propose possible neural mechanisms for enabling predictive coding in the brain, the actual circuit system has not been identified so far. In the following section, a possible implementation for PP in the human brain will be introduced.

1.3.1.2. Neural Mechanisms of Predictive Processing

Hierarchical organization appears to be a key principle in the structure of the brain. This is most visible in the visual system where lower primary areas receive the incoming sensory input while higher cortical areas play a role in the association of the visual input as well as connect different modalities in the brain.

Conjectural predictive coding circuits exploit this structure to implement a cortical organization that would facilitate predictive coding.

The neuronal activity that would be required for such a circuit is thought to take place in the neocortex of the brain. A possible coding scheme to implement predictive coding in the brain involves two functionally distinct subpopulations of pyramidal neurons in every cortical sensory region (Clark, 2013; Kok, 2015; Shipp, 2016). These two populations are characterized by their different computational roles and different connectivity patterns in the brain: backward projecting prediction units that represent the hypothesis that best explains the current sensory input in this region and forward projecting error units that carry prediction error. The latter represents the mismatch between the input and the current hypothesis. These units interact in order to find the best fitting hypothesis for the sensory input and thus reduce the prediction error (or the activity of the error units in the cortex) (Kok, 2015). The following rules apply:

Error units in one region serve as input to the next region in the cortical hierarchy

- Hypothesis gets altered to better fit bottom-up input
- A new hypothesis is sent back down as a prediction and is compared with the current hypothesis at the lower hierarchical level
- The mismatch between the two hypotheses forms a new prediction error which is sent back up to the next hierarchical level.

These steps as suggested by Kok (2015) are performed iteratively and constantly.

Shipp (2016) adds another sub-population of functionally distinct neurons to this framework. Along with the prediction units and the error units, he proposes precision units that weigh sensory input according to its reliability and saliency in order to increase efficiency in perception.

The neuronal dynamics implied by predictive coding require prediction units and error units to interact on each hierarchical layer as visualized in Figure 4. For a more detailed scheme see Shipp (2016).

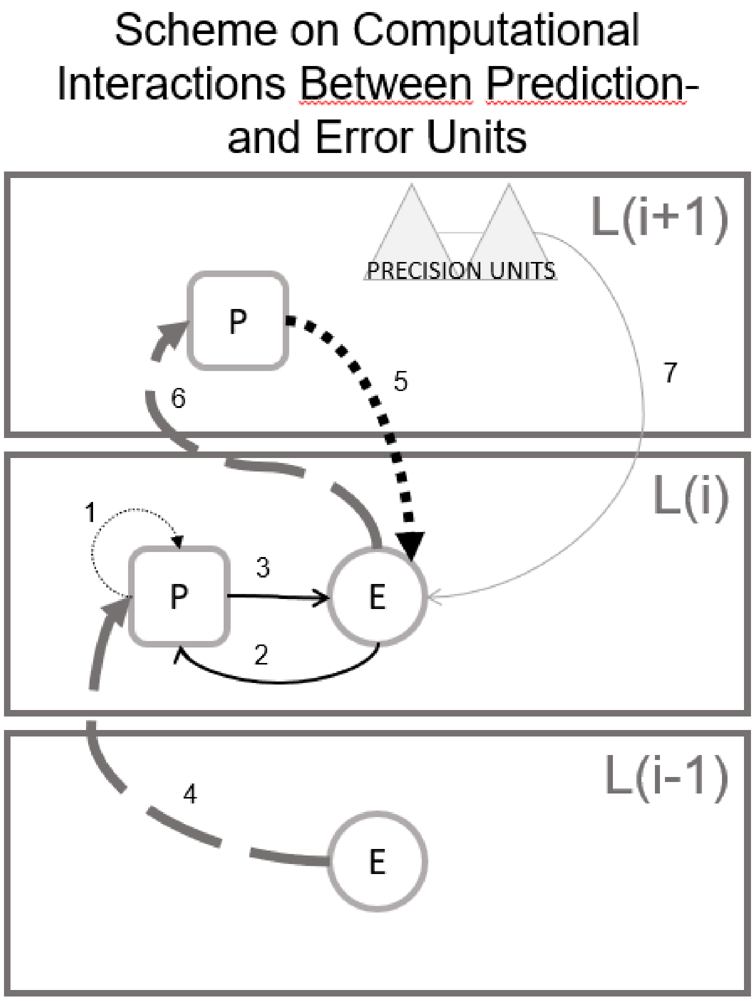

Figure 4: Simplified scheme on the interaction of prediction units and error units. Displayed on hierarchical level L(i) as adapted from Shipp (2016). Prediction units (P) recursively update themselves (1) with inputs from Error units (4,2). Error units (E) compare the activity of the associated expectation (3) with input of other prediction units (5) and send error signals to same level (2) and hierarchically higher prediction units (6). The gain of the error units is modulated by prediction units (7).

Predictive coding schemes typically assume a specific distribution of different unit types across the cortical laminae. Forward connections, which are thought to carry the error signal, arise predominantly in superficial pyramidal cells in layers I, II, and III and terminate on spiny stellate cells of layer four in higher cortical areas.

Prediction units have been associated with backward connections which arise largely from deep pyramidal cells in infragranular layers V and VI. These connections target cells in the infra- and supragranular layers of lower cortical areas. Additionally, there are intrinsic connections that are refined to the cortical sheet and involved in lateral interactions between close-by neurons. It is important to note that the terms ‘forward’ and ‘backward’ in this context refer to the neurons’ different laminar terminations (Friston, 2008). The neurons involved are excitatory pyramidal neurons which are connected by extrinsic corticocortical connections. However, the separation of forward and backward connections is not fully assigned to supragranular and infragranular layers.

Components of the forward connections have been found to originate in deep cortical layers whereas superficial layers give rise to forward as well as to backward connections (Shipp, 2016). Yet, in experiments with primates, it has been found that the different projections (forward and backward) are separate at a cellular level, thus extrinsically bifurcating axons do not project in both directions, providing the basis for neural circuity (Markov et al., 2014).

There is some debate as to whether the superficial component in the backward projection may be associated with precision signals (Shipp, 2016). Based on findings in rodents and primate cortex, Shipp further expanded the circuit proposed in Figure 4 and proposed a possible circuit for predictive coding in a mid-tier area in sensory cortex regions (Figure 5).

Figure 5 shows how superficial error units compare the expectation encoded at each level in the hierarchy with the descending prediction from the higher hierarchical level. The error units get excited by associated prediction units and inhibited by the descending prediction creating a subsequent inhibitory link from the error unit to the associated prediction units resulting in a negative feedback loop. This allows prediction signals to propagate backward across hierarchical levels by allowing the descending suppression of error to influence expectation units at the lower level. The transmission of descending prediction signals might be facilitated by interneurons (Shipp, 2016).

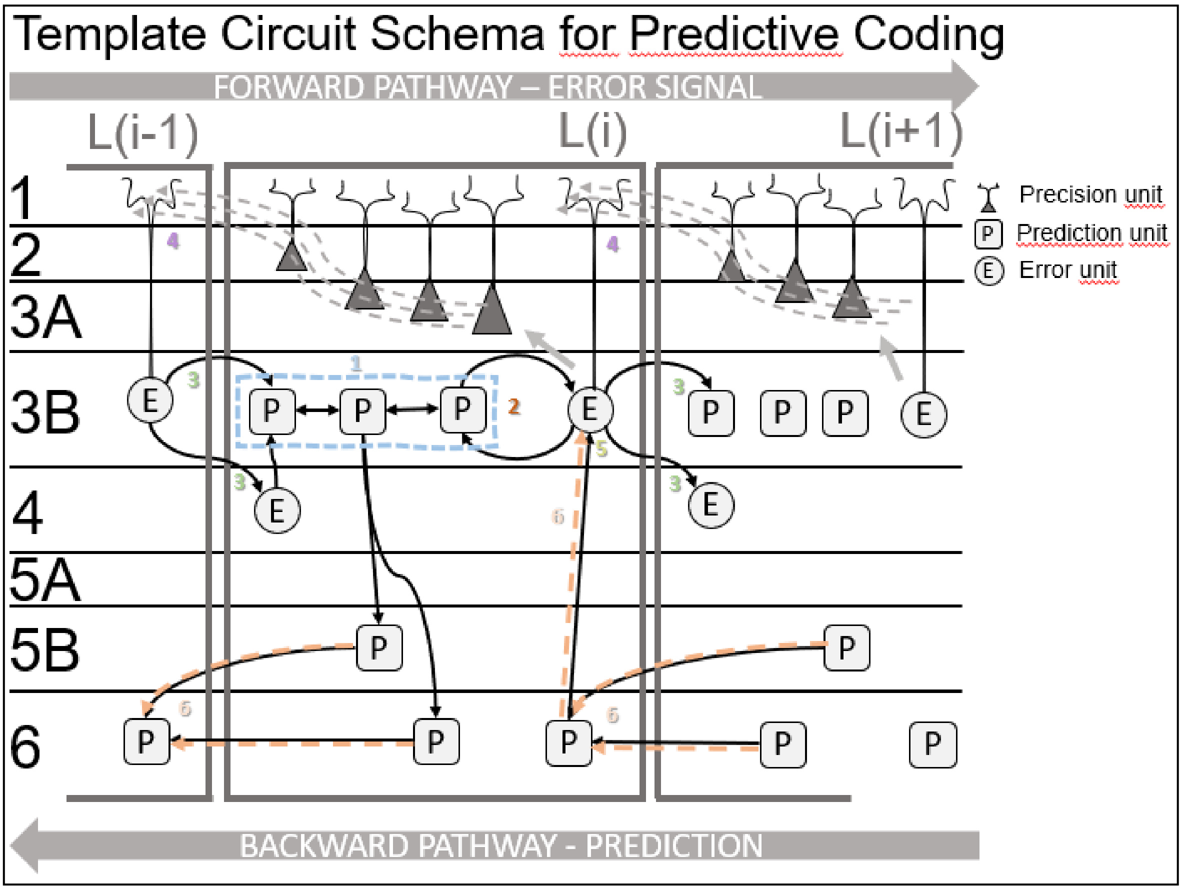

Figure 5: Simplified circuit diagram of a predictive coding circuit. Demonstrating how predictive coding could be implemented in cortical layers (1-6) for hierarchical layer L(i) adapted from Shipp (2016). Showing intrinsic and extrinsic connections between precision units (triangular), Prediction units (square) and error units (circular). Extrinsic forward connections terminate in layers 4 and 3B (pathway 3). Networked prediction units (1) get excited by ascending error signals (3) and inhibited by local error unit (5) in layer 3B. The local error unit (5) in turn is excited by their associated networked prediction units (1) creating a negative feedback loop (2). The local superficial error unit (5) subtracts the excitatory input from the networked prediction units (1) with the descending prediction relayed by local interneurons which contact deep pyramidal neurons (6). Precision signals arise in superficial layers 2 and 3A and form a descending precision signal which modulate pyramidal error units.

1.3.1.3. Predictive Processing and Visual Perception

When looking at visual perception within the PP framework, the hierarchy which is essential to PP can be found in the visual system, since the way visual information gets processed in the brain appears to be hierarchical itself and different visual regions in the neocortex have different roles in visual processing.

Assumptions are that there is hierarchical predictive coding within each cortical region (Kok & de Lange, 2014) as well as within a hierarchy that includes most cortical regions involved in visual processing (Summerfield & Egner, 2009).

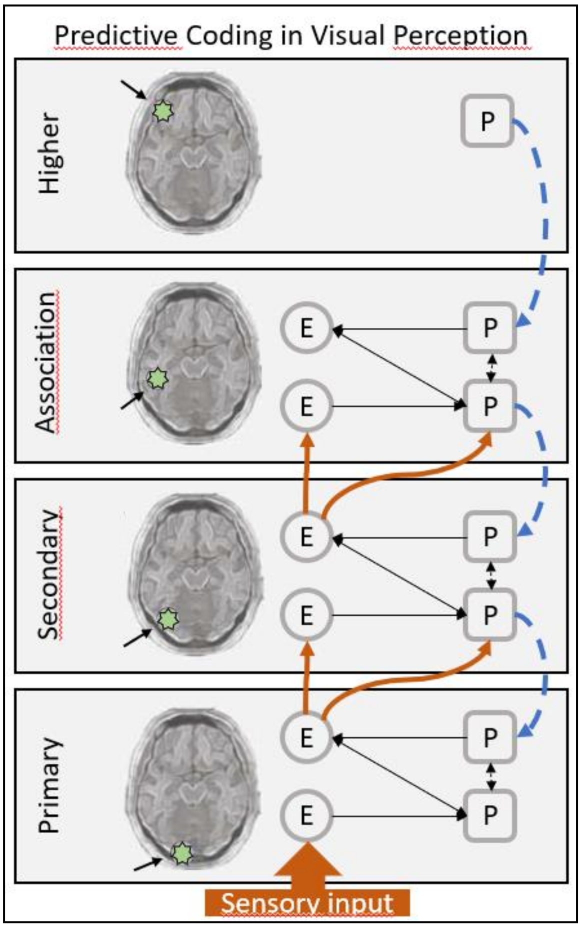

Figure 6: Simplified scheme on predictive coding in visual perception. Adapted from Summerfield & Egner (2009). Predictions descend the hierarchy (Blue, dashed arrow) in the visual system from higher cortical areas down the hierarchy to the primary visual cortex. At each level in the hierarchy prediction and sensory input (or prediction error) are compared to the local prediction by interactions between local error (circle) and prediction (square) units (interactions indicated by black arrows). The resulting prediction error is used to update the prediction in the higher hierarchical level (red arrow).

Predictions would be generated in higher cortical regions where the prior information is stored and fed backward to modulate the perceptual processing in lower sensory cortical regions. Figure 6 shows a simplified diagram of how higher areas pass down predictions to the lower cortical regions in iterative interactions with error signals that ascend the hierarchy. This is supported by studies that show that the inactivation of higher cortical regions alters the neural response in lower regions (Hupé et al., 1998).

1.4. Summary

Myopia is known to cause lower visual acuity at a farther distance, depending on the degree of myopia. This loss in visual acuity can be compensated with optical correction, normally contact lenses or glasses with concave lenses which help to focus the light on the retina. Some myopic individuals, however, choose not to wear optical correction regularly and on a daily basis, hence they have to manage with blurry visual input most of the waking time which can be considered less reliable information. This requires the myopic individual to constantly perform more ‘guesswork’ and active inference in order to make sense of the visual input. Within the predictive processing framework, this would result in a stronger role of top-down processes and greater demand on the cortical areas involved in prediction making (Kok, 2015).

Cortical thickness has been shown to vary depending on how intense and frequent an area is engaged in specific tasks (Engvig et al., 2010). Accordingly, the guiding research question for this thesis is the question of whether decreased visual acuity in subjects with uncorrected myopia is related to changes in the cortical thickness in these subjects.

2. Aim of the Thesis

This thesis aims to investigate differences in cortical thickness in individuals with low visual acuity and view the results within the theoretical framework of predictive processing theories. Therefore, to answer the research question of whether decreased visual acuity is associated with changes in cortical thickness, an MRI experiment was conducted to scan and analyze the thickness in parietal and occipital cortex regions which are known to be involved in visual processing.

Differences in cortical thickness in these regions were measured in participants with uncorrected myopia and poor visual acuity and compared to a myopic and an emmetropic control group that both report good visual acuity.

Accordingly, we hypothesized that subjects with uncorrected myopia show increased cortical thickness in the parietal cortex regions, an area which is repeatedly shown to be involved in top-down visual processing and suggested to play a role in generating prediction signals as discussed in the previous chapters on predictive processing and visual perception and the association cortex.

We further expected the thickness of the occipital cortex to not show any differences between the three groups since we expected cancelling out effects of stronger top-down and weaker bottom-up influences.

The following chapter will explain the experimental design that was used to investigate this question in detail.

3. Materials and Methods

To answer the research question, an extensive study was conducted at the Institute of Psychology at the Karl-Franzens-Universität in Graz in Austria.

3.1. Participants

Participants were recruited through the student mailing list of the University and social media. A total of sixty participants took part in the MRI study. In return for their time and effort, participants were offered monetary reimbursement and psychology students could alternatively receive study credits. The study was conducted in accordance with the Declaration of Helsinki and approved by the Ethics Commission of the University of Graz.

Prior to participation, volunteers were required to complete an online pre-screening questionnaire. The questionnaire took about 5 minutes, was based on the participant's self-report, and was written in the German language. Questions were grouped into three blocks. In the first block, participants were asked to fill in their socio-economic information, namely, their age, gender, occupation, and educational attainment level.

The second block contained questions about the participant's ophthalmic history, possible vision deficits, and whether the participant wears optical correction as well as the subjective evaluation of the individual visual acuity. The third block contained information about the study procedure, MRI contraindications, and participants were asked whether they meet the MRI safety requirements.

Participants were excluded from the study if they reported ophthalmologic disorders other than myopia that led to decreased visual acuity. This also applied to refractive errors like strong astigmatism or hyperopia as well as strabismus or impaired depth perception. Other exclusion criteria were a history of neurological or cardiovascular diseases, the intake of medications with an effect on the central nervous system as well as not meeting the general MRI-safety criteria which comprise conditions like claustrophobia, not MR-compatible grafts, pacemakers, insulin pumps, middle ear implants, cardiorespiratory or orthopedic disorders, neuropsychological/sensory impairment, etc.

Over 300 people filled out the questionnaire and 250 were suitable for the study.
In order to investigate the research question, the participants were assigned to one of three experimental groups, based on their responses in the pre-screening questionnaire. For the assignment, attention was paid to the equal distribution of age and gender in all groups.
The first group contained participants that were myopic but chose not to wear optical correction in their everyday life other than short periods of time that require good vision like driving a car or during class. For this group, the time that the optical correction was used had to be less than 10% of the waking time. Additionally, myopic participants who wore optical correction frequently but whose myopia was insufficiently compensated by their glasses or contact lenses and who reported poor vision while wearing their optical correction were also included in this group. It is important to note that participants with ophthalmologic disorders that could affect visual acuity other than myopia were excluded from the study beforehand.

The second group two was a control group that was composed of participants that were myopic but wore their glasses or contact lenses frequently and more than 50% of their waking time with their myopia sufficiently compensated to ensure good vision when wearing their optical correction.

The third group consisted of participants who reported good vision, good visual acuity, and no subjective need for optical correction. Furthermore, participants who were myopic in the past but underwent refractive surgery in the past were also included in this group.

To confirm the assignment to the right group, a vision test was performed in a separate session to obtain an objective measure of the participant’s far acuity. This was done using The Freiburg Visual Acuity and Contrast Test (Bach, 1996). This computerized test uses Landolt-C optotypes which are displayed in one of eight orientations. Participants had to indicate the perceived orientation via a keyboard.

The test was performed for each eye separately and later with binocular vision and both eyes open.

3.2. Data Acquisition

MRI data was acquired using a 3-Tesla MRI Siemens Magnetom Vida scanner (Siemens, Erlangen, Germany), located at the Technical University of Graz. Prior to the MRI examination participants were asked to sign an informed consent form and an MRI safety screening form and were instructed about the procedure.

The participants each underwent a series of measurements that took about 80-90 minutes in total.

- Localizer scan (00:00:14)
- T1-weighted structural scan (00:06:03)
- T2*- weighted functional (resting state) scan (00:08:22)
- T2*-weighted functional (field map) scan (00:00:03)
- T2*- weighted (task-based) fMRI scan (00:05:19)
- T2*-weighted functional (field map) scan (00:00:03)
- T2*-weighted (task-based) fMRI scan (00:05:19)
- T2*-weighted functional (field map) scan (00:00:03)
- Diffusion-weighted scan (00:01:51)
- T2*-weighted functional (field-map) scan (00:00:22)
- Diffusion-weighted scan (00:03:42)
- T2*-weighted functional (field-map) scan (00:00:26)
- 4 high-resolution scans (each 00:07:11)
- T2*-weighted structural scan (00:05:22)

For this thesis, only the T1-weighted magnetization-prepared rapid gradient echo (MP-RAGE) structural scans were used.

The T1-weighted structural scan had the following acquisition parameters:

- 176 slices
- Voxel size: 1 mm3 isotropic
- TR = 2.53 s
- TE = 3.88 ms
- TI = 1.2 s
- flip angle = 7°
- FOV= 263x350 mm

3.3. MRI Data Analysis

The data was analyzed using FreeSurfer Software Suite for Linux version 6.0.1. (FreeSurfer, 2021) using the standard recon-all processing pipeline as a part of fMRIprep version 1.580.2.16. This processing stream consists of several steps and serves to automatically reconstruct the volumetric segmentation as well as the cortical surface (Reuter et al., 2012). Briefly, the steps in the pre-processing stream comprise motion correction, Talairach transformation, several stages of intensity normalization, and skull stripping. After that, the white matter was segmented and the boundary marked in order to reconstruct the gray and the white matter. Also, an algorithm was applied to the volumes and cortical regions for them to undergo a labelling process. At this point, FreeSurfer automatically measures the cortical thickness of each subject and generates cortical thickness maps. Here, the cortical thickness is defined at each vertex as the average of the shortest distances between the gray- and white matter boundary and the pial surface (Dale et al., 1999; Fischl & Dale, 2000).

3.4. Proband Information

To control for differences in cortical thickness due to age differences between the three experimental groups, the participant’s mean age for each group was calculated and compared to the other groups using the Kruskal-Wallis test.

3.4.1. Visual Acuity Data

The participant's performance on the Freiburg Visual Acuity and Contrast Test was analyzed using the Kruskal-Wallis test to find out if the difference between groups was significant. The relationship was further examined using paired Wilcoxon test. This was done for all three conditions: binocular visual far acuity and far acuity tests for the right and the left eye separately.

3.5. Whole-brain Analysis

The first part of the data processing focussed on group analysis of the cortical thickness differences between the three experimental groups. This was done following the FreeSurfer protocol and instructions for group analysis (Fischl & Dale, 2000).

Before starting with the group analysis, the data was assembled into one file. This was done by resampling each subject into a common space. Subsequently, the data was smoothed, making use of a 10 mm full-width half-maximum (FWHM) Gaussian filter. The size of the filter proved beneficial for statistical power as demonstrated by Liem and collaborators (2015).

In the next step, a general linear model (GLM) analysis was performed at each surface location (vertex) of the cortex to compare thickness between the three groups. For a detailed description of the FreeSurfer processing steps see Fischl and Dale (Fischl & Dale, 2000).

In order to detect statistically significant differences in cortical thickness, an F-Test test was conducted.

To control for false-positive results due to multiple comparisons, cluster-wise correction for multiple comparisons was performed after every statistical test. This was achieved by running a permutation simulation to get a measure of the distribution of the maximum cluster size under the null hypothesis. The simulation consisted of 1000 iterations. The cluster forming vertex-wise threshold was set to 4 ($p=0.0001$) to detect clusters in the threshold map. Only clusters with significant cluster-wise p values ($p\leq0.05$) were preserved.

Later, the vertex-wise threshold was set to 1.3 (p=0.05) to also detect less significant clusters.

These simulations were run several times to compare different groups and effects

- Group 1 (uncorrected myopic) vs. Group 3 (emmetropic)
- Group 1 vs. Group 2 (corrected myopic controls)
- Group 2 vs. Group 3
- Group 1 vs. Group 2+3

3.6. Regions of Interest

The second part of the data processing focused on the region of interest (ROI) analysis. For the ROI analysis, we made use of the probabilistic atlas of visual topographic areas by Wang and collaborators in FreeSurfer fsaverage standard surface space (Wang et al., 2015). We purposefully chose to use a probabilistic map of the cortical surface because of its superior properties in identifying relevant regions involved in visual processing.

We focussed on two main types of topographic regions:

- occipital cortex: early visual areas (area V1-V3)
- Parietal cortex areas: higher-level topographic areas of the intraparietal sulcus (IPS 0-5)

13 ROIs defined in the probabilistic atlas by Wang and collaborators (2015) were summarized to 10 ROIs, combining the ventral and dorsal portions of V1, V2 and V3 which were previously defined as one ROI each. Furthermore, 3 additional ROIs were added to the analysis, that proved relevant for visual activity in prior studies by Zaretskaya and colleagues (2013).

3.6.1. Definition

In this study, the atlas of the human topographic visual areas by Wang and collaborators (2015) was used to parcellate the cortical surface into 25 regions of interest that are involved in visual processing (Figure 7). This atlas is a probabilistic atlas that defines the likelihood of a given coordinate on the cortical surface being associated with a given functional region. This helps to control for anatomical and functional variability across individual subjects (Wang et al., 2015). In this thesis, we focus on early visual areas V1-V3 as well as the parietal areas IPS0-IPS5.

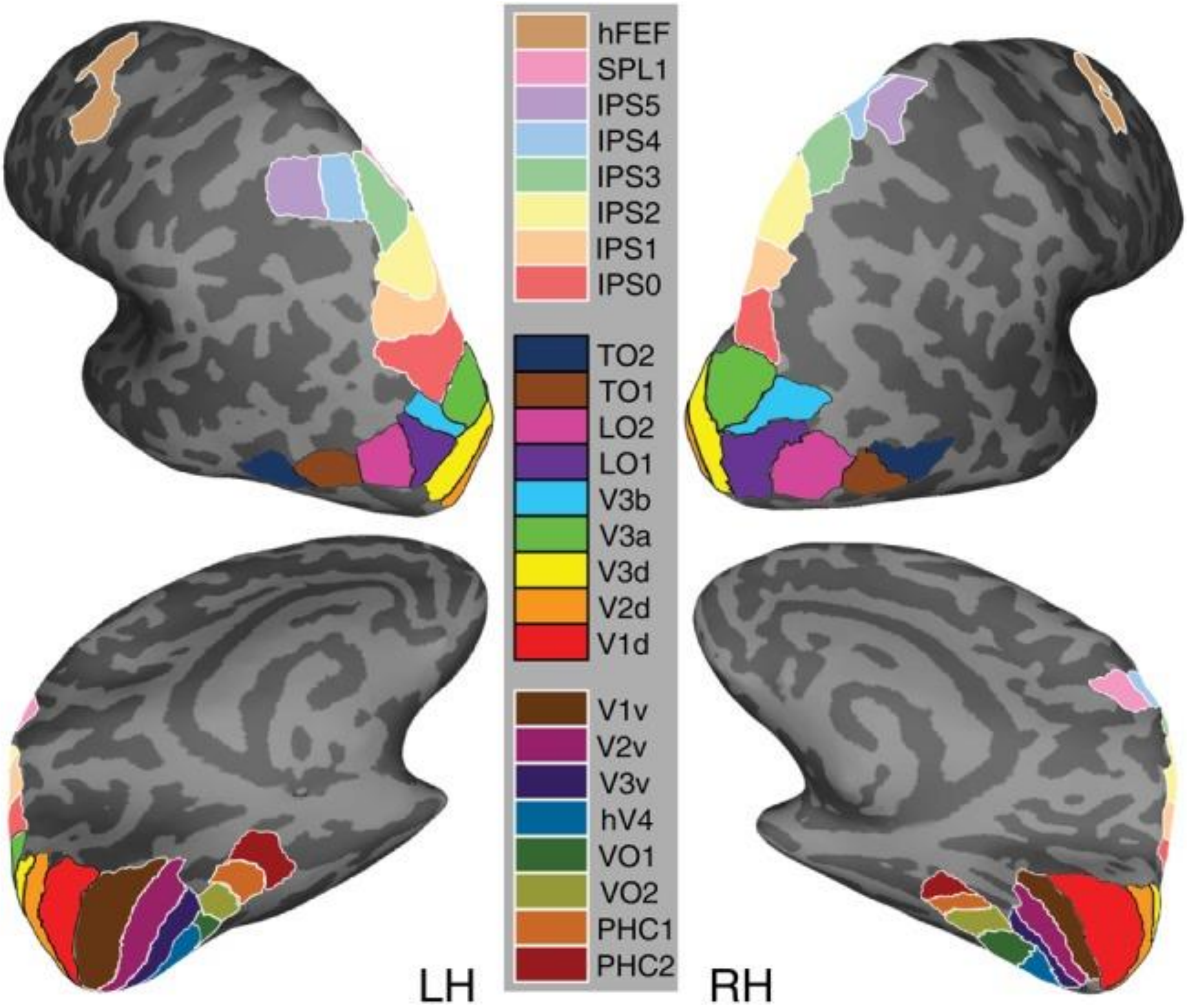

Figure 7: Schematic borders of 25 topographic visual regions. Displayed on a representative subject. The areas outlined on the inflated cortical surface were delineated in individual subjects and used to generate the surface-based atlas (Wang et al., 2015).

3.6.1.1. Early Visual Areas

The early visual areas consist of six topographic areas in the posterior occipital cortex. In the atlas, the ventral and dorsal portions of V1, V2, and V3 were defined separately so that ventral ROIs carry the representation of the upper contralateral visual field and the dorsal ROIs of the lower contralateral visual field (Wang et al., 2015).

The ventral ROIs start with ventral V1 (V1v), which extended from the horizontal meridian in the fundus of the calcarine sulcus to an upper vertical meridian that forms the border of V1v and ventral V2 (V2v). From there, V2v continues to a horizontal meridian that forms the border to ventral V3 (V3v). V3v borders with V4 and the ventral occipital cortex region I (VO1) (Wang et al., 2015).

The dorsal ROIs start with dorsal V1 (V1d), which stretches from the calcarine sulcus to a lower vertical meridian that forms the border with dorsal V2 (V2d). V2d again stretches to a horizontal meridian where dorsal V3 (V3d) starts. V3d meets borders with V3 A and V3 B and lateral occipital cortex region I (LO1). All of these areas (V1-V3) share a foveal confluence (Wang et al., 2015).

Since ventral and dorsal portions *of* V1-V3 form a complete representation of a hemifield, for this thesis, we combined ventral and dorsal portions of each area into V1, V2, and V3.

3.6.1.2. Parietal Regions

Concerning the parietal region of the human cortex, the atlas identifies 7 regions involved in visual processing. Six regions are located along the intraparietal sulcus (IPS0/ V7, IPS1-5) and one in the superior parietal lobule (SPL1) (Wang et al., 2015). These areas correspond to what is often referred to as the ‘dorsal pathway’ in visual processing.

3.6.1.2.1. Anatomical location

V7 or IPS0 is localized along the transverse occipital sulcus and exhibits a retinotopic representation of the contralateral visual hemifield. IPS1-IPS4 each contain a representation of the contralateral visual field and have been distinguished using spatial attention, saccade, and fixation tasks. IPS5 is located at the intersection of the intraparietal and postcentral sulcus. Based on the anatomical location and topographic organization, IPS5 may correspond to the ‘parietal face area’ described by Sereno and Huang (2006). Finally, SPL1 refers to an area on the superior parietal lobule that was also found to be active during these tasks (Konen & Kastner, 2008).

3.6.1.2.2. Function

The topographic parietal areas show differential functional responses. For example, IPS1 has been found to be activated by saccadic eye movements and reaching movements, whereas IPS2 primarily responds to reaching tasks. IPS1-3 showed stronger activation in radial motion than in planar motion whereas IPS4, IPS5, and

SPL1 showed no motion preference (Konen & Kastner, 2008). Furthermore, IPS1 and IPS2 have been found to exhibit object-selective responses which were not present in IPS3 and IPS4 (Konen & Kastner, 2008).

Differences between the parietal topographic maps were also observed in their responses to eye movements. Areas IPS1, IPS2, and SPL1 reacted to saccadic eye movements more, whereas IPS3, IPS4, and IPS5 exhibited preferential responses evoked by smooth pursuit eye movements (Konen & Kastner, 2008). Overall, the activity related to eye movements that was observed along the IPS showed a rather gradual representation concerning the different types of eye movements. Responses for saccades and small pursuit eye movements increase from posterior/medial to anterior/lateral with the greatest preference for saccades in SPL1 and smooth pursuit in IPS5.

The probabilistic atlas by Wang and collaborators (2015) contains 12 other regions that are involved in visual processing. These regions are mainly located in the ventral-temporal, the dorsal-, lateral-, and temporal-occipital cortex. However, these regions are not part of the research question that guides this thesis, and there is no hypothesis for these regions. Thus, we chose to not consider them in our analysis.

3.6.1.3. Further Regions of Interest

In addition to the regions identified in the probabilistic atlas, three more ROIs were added to the analysis. These ROIs were identified based on the fMRI results of Zaretskaya and collaborators (2013) and comprise the anterior intraparietal sulcus, the superior parietal lobule, and the early visual areas. These regions have been repeatedly identified in fMRI experiments during the processing of bistable visual illusions (Grassi et al., 2016).

The anterior intraparietal sulcus (aIPS) as defined by Zaretskaya and colleagues (2013) has been linked to visual attention and attentional selection in former studies (Corbetta & Shulman, 2002). In their study, they showed the involvement of aIPS in gestalt perception and perceptual grouping. The anatomical location and coordinates were identified using fMRI (Figure 8).

The superior parietal lobe region used in Zaretskaya and colleagues (2013) differs in its anatomical location from the ROI SPL1 defined by Wang and collaborators

(2015) in their atlas, overlapping with parts of the IPS3 and IPS4 regions (Figure 8). Therefore, it will be referred to as 'SPL0' in this thesis. SPL0 also showed involvement and significant peaks during Gestalt perception tasks in fMRI scans (Zaretskaya et al., 2013).

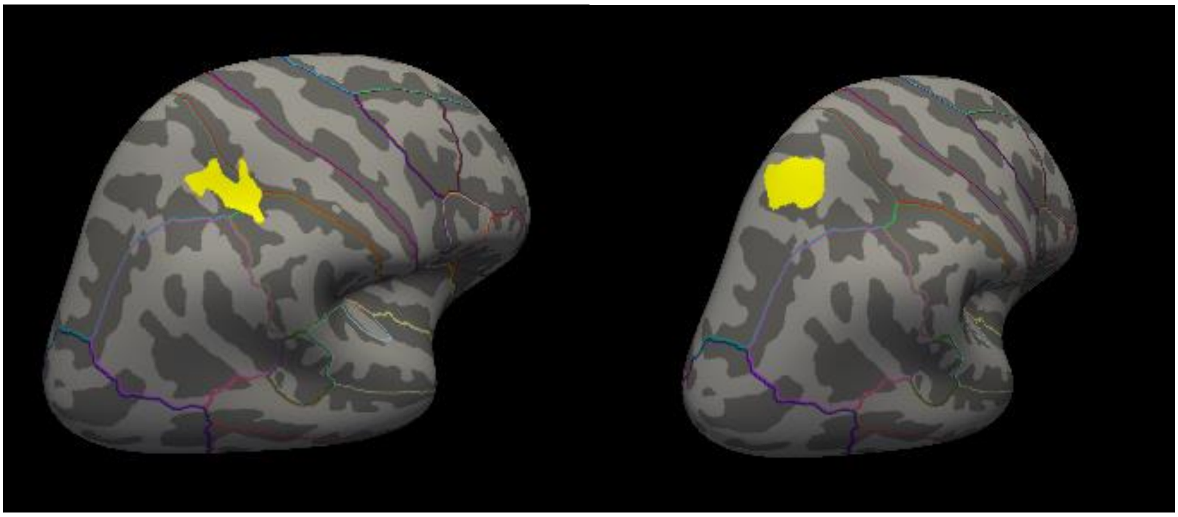

Figure 8: Locations of ROI aIPS and SPL0 on the tight hemisphere. Left: aIPS, right: SPL0, here marked in yellow, as displayed in the FreeSurfer visualisation tool Freeview on the right hemisphere.

The last ROI that was used refers to early visual areas that showed deactivation during Gestalt perception (Zaretskaya et al., 2013). This region will be referred to as 'visual' in this study. The anatomical location corresponds with the early visual areas in the probabilistic atlas by Wang and collaborators (2015) as can be seen in Figure 9.

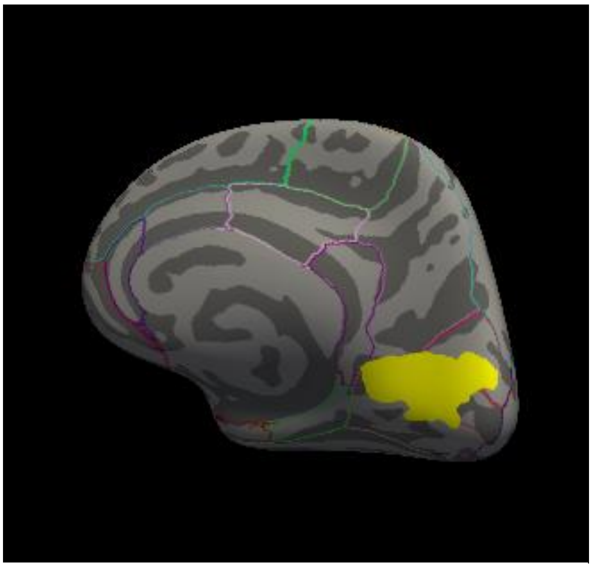

Figure 9: Location of visual ROI. ROI marked in yellow, as displayed in FreeSurfer's Freeview on the right side.

Analysis was performed for each hemisphere separately. Figure 10 shows the 13 ROIs defining the area on the cortex that was analyzed.

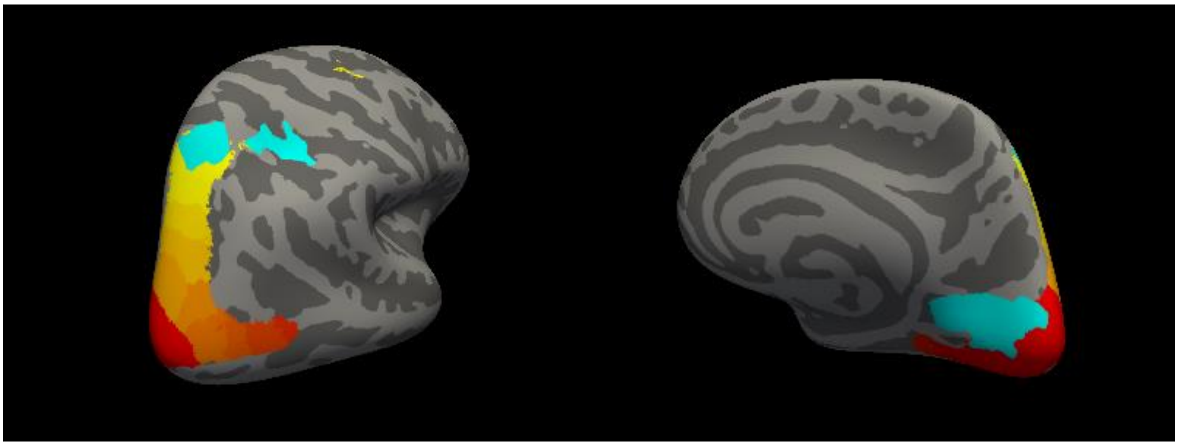

Figure 10: Complete ROIs used for analysis. ROIs visualized on the right hemisphere. ROIs V1, V2, V3, IPS0-5, SPL1 from Wang et al. (2015) displayed in shades of orange, aIPS, SPL0 and evisual from Zaretskaya et al. (2013) in turquoise.

3.6.2. ROI Analysis

In the consecutive step, the average thickness in these ROIs was calculated using FreeSurfer mri_segstats command and the resulting cortical thickness values were printed into a table.

In order to meaningfully answer the research question and to examine the difference in cortical thickness between the three experimental groups, statistical analyses and significance testing were performed on the values using R Studio (RStudio, 2021). After testing for normality using the Shapiro-Wilk test, one-way ANOVA or Kruskal Wallis test were performed on the data set to analyze it for significant differences between groups. Afterwards, post hoc tests in the form of paired T-tests for the normally distributed data and pairwise Wilcoxon tests for the non-normally distributed data were performed for each ROI.

Following our hypothesis, we were looking for an effect such that Group 1 is significantly different from Group 2 and Group 3, but the effect is not present between Group 2 and Group 3.

3.7. Regression Analysis

Lastly, in addition to group analysis, a regression analysis was performed to investigate the relationship between cortical thickness in all the ROIs and participants' visual acuity performance in the Freiburg Visual Acuity and Contrast Test over all participants (irrespective of the group assignment), with age- as well as their gender as covariates. We did this to compensate for potential erroneous group assignment of participants, which was based on their self-report. Regression was performed for each hemisphere separately using FreeSurfer software. Subsequently, multiple comparison correction and small volume correction were performed on the data to control for false-positive results.

4. Results

Out of 300 volunteers that applied for participation in the study, a total of sixty subjects were recruited for the MRI scanning, 37 were female and 23 were male. The majority of participants were students (80%).

Group 1 contained 19 myopic subjects who chose not to wear optical correction for more than 10% of the waking time. Additionally, this group contained participants who had their myopia insufficiently compensated with an optical correction that was too weak for their needs according to their self-report. Average myopia in this group was 1.42 dpt for the right eye and 1.46 dpt for the left eye. However, the median value for the left and the right eye was 0.5 dpt 7 out of 19 participants did not know the exact degree of their short-sightedness. The average measured visual acuity in Group 1 was 0.07 logMAR for the right eye and 0.03 logMAR for the left eye according to the Freiburg Visual Acuity and Contrast Test. When examining binocular visual acuity, the average value in this group was -0.07 logMAR.

Group 2 was the myopic control group and contained 18 myopic subjects who wore their optical correction frequently and on a daily basis and more than 50% of their waking time. Here, the average diopters for the right eye were -2.39 dpt and for the left eye, the value was -2.28 dpt The average visual acuity in this group with participants using their optical correction was -0.12 logMAR for the right eye and -0.10 logMAR for the left eye. When testing the binocular condition, the average visual acuity was -0.20 logMAR.

In the emmetropic group, Group 3, there were 23 individuals. The average visual acuity here was -0.06 logMAR for the right eye and -0.07 logMAR for the left eye. With both eyes open, the average visual acuity in Group 3 was -0.20 logMAR.
The performance on the Freiburg Visual Acuity and Contrast Test for each experimental group and each condition is shown in Figure 11 and Figure 12.

Concerning the participant’s age, the mean overall age was 24.03 years (SD=3.16). The mean age in Group 1 was 23.89 years (SD=2.96), in Group 2 it was 23.61 years

(SD=2.77) and in Group 3 it was 24.48 (SD=3.72). When statistically comparing the three groups using Kruskal-Wallis Test (KWT), the difference in age was not significant for any group constellation with a weak effect (KWT, p=0.847, η²= 0.029)(Cohen, 1988).

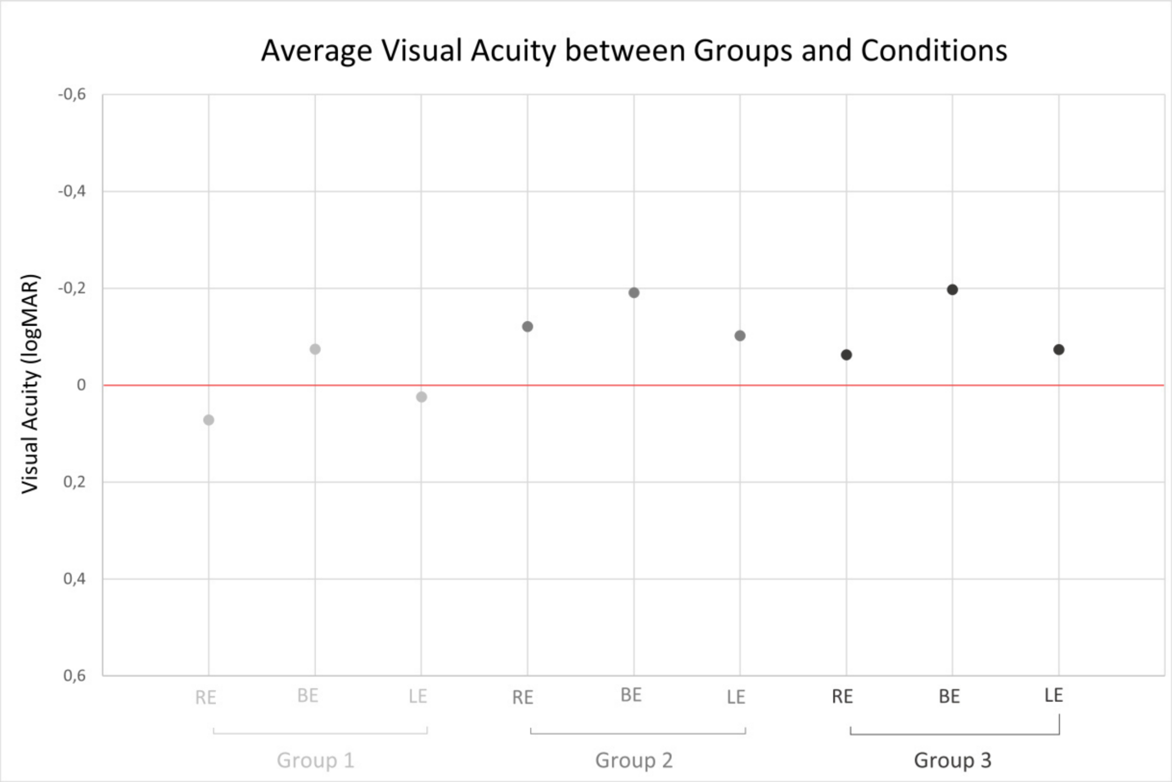

Figure 11: Mean performance on the Freiburg Visual Acuity and Contrast Test for each condition in each group. RE = right eye, BE = both eyes, binocular condition, LE = left eye. "0" marks normal visual acuity.

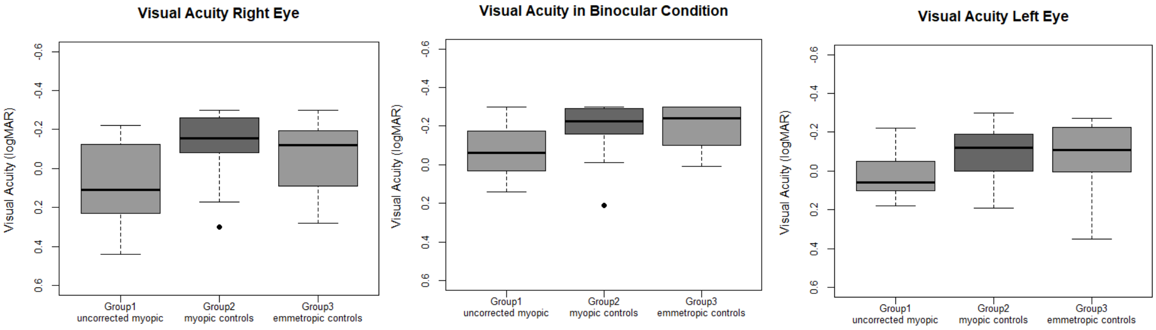

Figure 12: Boxplots displaying the visual acuity scores for each experimental group in each testing condition.

4.1. Visual Acuity Data

Comparing the visual acuity data across groups using Kruskal-Wallis tests, we find that there is a significant difference in visual far acuity for the right eye, the left eye, and the binocular acuity when comparing Group 1 (uncorrected myopic) and Group 2 (myopic controls) as well as Group 1 and Group 3 (emmetropic). The difference in visual acuity is not significant between Group 2 and Group 3 (see Table 1 for a complete description of the statistical results).

Statistical Analysis of Visual Acuity between Groups

	Kruskal-Wallis Rank Sum Test	**Pairwise Wilcoxon Test** p-Value difference between groups		
Condition	between all groups	Groups	1	2
Binocular	$p= 0.007, \eta^2= 0.14$	2	p=0.022, r=0.296	-
		3	p=0.012, r=0.323	p=0.852, r=0.024
Right	$p= 0.016, \eta^2= 0.109$	2	p=0.019, r=0.304	-
		3	p=0.092, r=0.218	p=0.330, r=0.126
Left	$p= 0.012, \eta^2= 0.122$	2	p=0.009, r=0.335	-
		3	p=0.049, r=0.254	p=1.000, r=0.001

Table 1: Analysis of visual acuity between groups. Results from performing KWT and pairwise Wilcoxon test on performance on the visual acuity test in all three conditions: binocular condition, visual acuity test with the right eye, and with the left eye.

4.2. Whole-brain Cortical Thickness

Cortical thickness differences between groups were tested using a one-way ANOVA at each surface location (vertex) of each hemisphere. This analysis revealed multiple significant clusters (Figure 13). However, those clusters did not survive the correction for multiple comparisons. Hence, in the whole-brain analysis, no significant differences in cortical thickness between the three groups were found.

Contrast of Group 1 with Groups 2 & 3: Significance Map of Differences in Cortical Thickness after One-way ANOVA, Before Correction for Multiple Comparisons *(p= .05)*

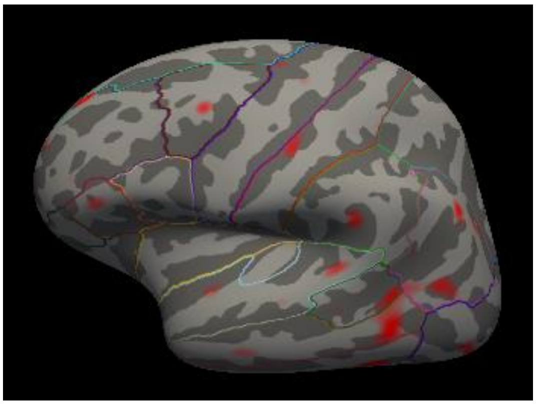
Figure 13.1: LH, lateral view

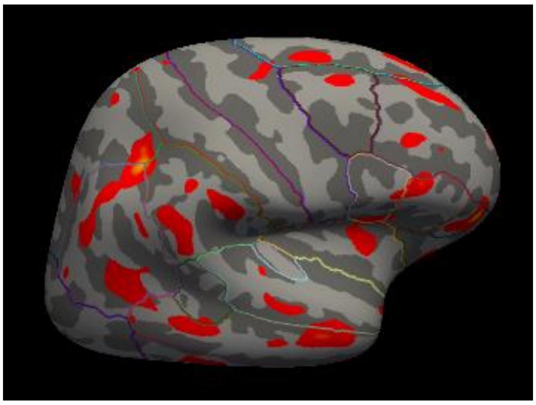
Figure 13.1: RH, lateral view

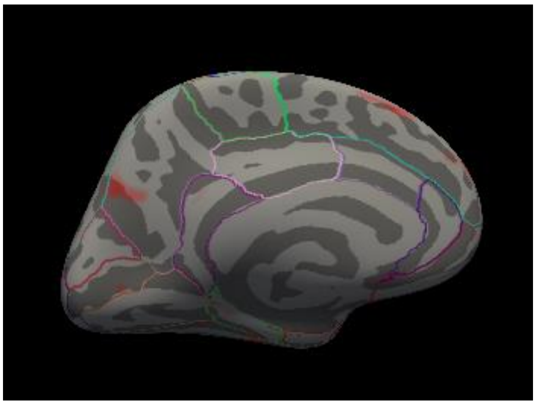
Figure 13.3: LH, medial view

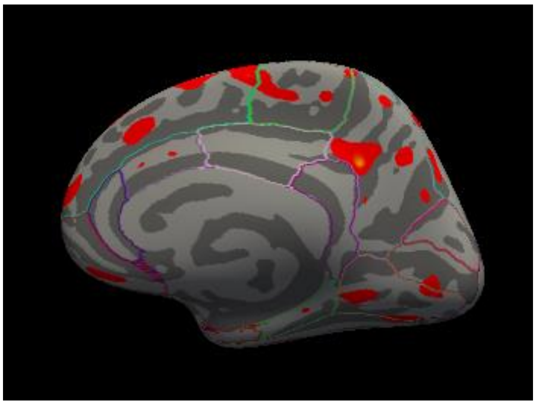
Figure 13.4: RH, medial view

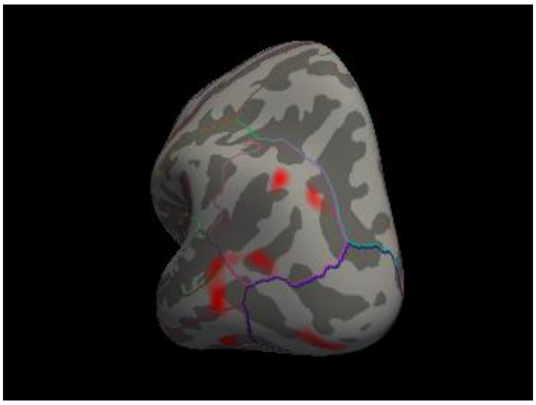
Figure 13.5: LH, dorsal view

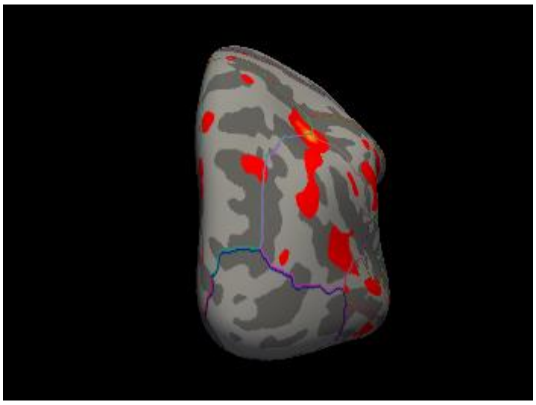
Figure 13.6: RH, dorsal view

Figure 13.1 – 13.6: Whole-brain results contrasting Group 1 with controls. Significant differences in cortical thickness in the left and right hemisphere before multiple cluster correction when contrasting Group 1 with the other two groups in lateral, medial, and dorsal view. RH = right hemisphere, LH = left hemisphere.

4.3. ROI Analysis

All 13 ROIs were analyzed and compared between groups. Table 2 shows the mean cortical thickness values and the standard error for each group in every ROI and hemisphere.

Only two of the 13 regions showed a significant difference in thickness between the three groups.

Mean Cortical Thickness (mm) and Standard Error for each Group and ROI

			IPS0	IPS1	IPS2	IPS3	IPS4	IPS5	SPL1	V1	V2	V3	SPL0	aIPS	evisual
Left	Group1	mean	2.333	2.295	2.335	2.411	2.275	2.048	2.604	1.694	1.853	2.125	2.482	2.238	2.110
		St.error	0.151	0.167	0.172	0.247	0.218	0.402	0.376	0.126	0.100	0.187	0.189	0.354	0.096
	Group2	mean	2.291	2.215	2.290	2.444	2.244	2.115	2.510	1.690	1.868	2.081	2.411	2.239	2.099
		St.error	0.138	0.210	0.144	0.279	0.203	0.345	0.386	0.118	0.124	0.128	0.184	0.276	0.092
	Group3	mean	2.264	2.249	2.296	2.463	2.266	2.155	2.581	1.707	1.867	2.113	2.402	2.203	2.069
		St.error	0.161	0.157	0.207	0.325	0.302	0.359	0.369	0.141	0.126	0.140	0.325	0.258	0.097
Right	Group1	mean	2.348	2.317	2.287	2.383	2.228	2.398	2.605	1.774	1.854	2.164	2.448	2.319	1.741
		St.error	0.205	0.170	0.184	0.176	0.278	0.462	0.315	0.129	0.107	0.165	0.209	0.184	0.100
	Group2	mean	2.347	2.247	2.210	2.278	2.152	2.206	2.355	1.735	1.851	2.091	2.342	2.233	1.724
		St.error	0.163	0.214	0.199	0.209	0.287	0.312	0.296	0.116	0.113	0.122	0.204	0.091	0.108
	Group3	mean	2.294	2.258	2.169	2.372	2.273	2.339	2.548	1.772	1.894	2.117	2.380	2.176	1.736
		St.error	0.182	0.167	0.205	0.217	0.361	0.430	0.378	0.155	0.136	0.130	0.241	0.153	0.115

Table 2: Mean cortical thickness (mm) and standard error for each group and each ROI. Results displayed for each hemisphere.

The ROI superior parietal lobe (SPL1) showed a significant difference between groups (KWT, p= 0.02, η²= 0.102) and moderate effect size (Cohen, 1992) when running the Kruskal-Wallis-Test in the right hemisphere only (Tomczak & Tomczak, 2014). The consecutive post-hoc Pairwise Wilcoxon Rank Sum Test (WRST) showed significantly higher thickness values in Group 1 compared to the myopic control Group 2 with a large effect size (WRST, p= 0.014, η²=0.318). However, Group 1 was not significantly different from Group 3, showing a small effect size (p= 0.638, η²= 0.061). Group 2 and 3 showed a non-significant difference with a large effect size, with a trend towards higher thickness values in Group 3 (p= 0.095, η²=0.215) (Figure 14). Hence, we cannot reject the null hypothesis of no difference between the groups for the SPL1.

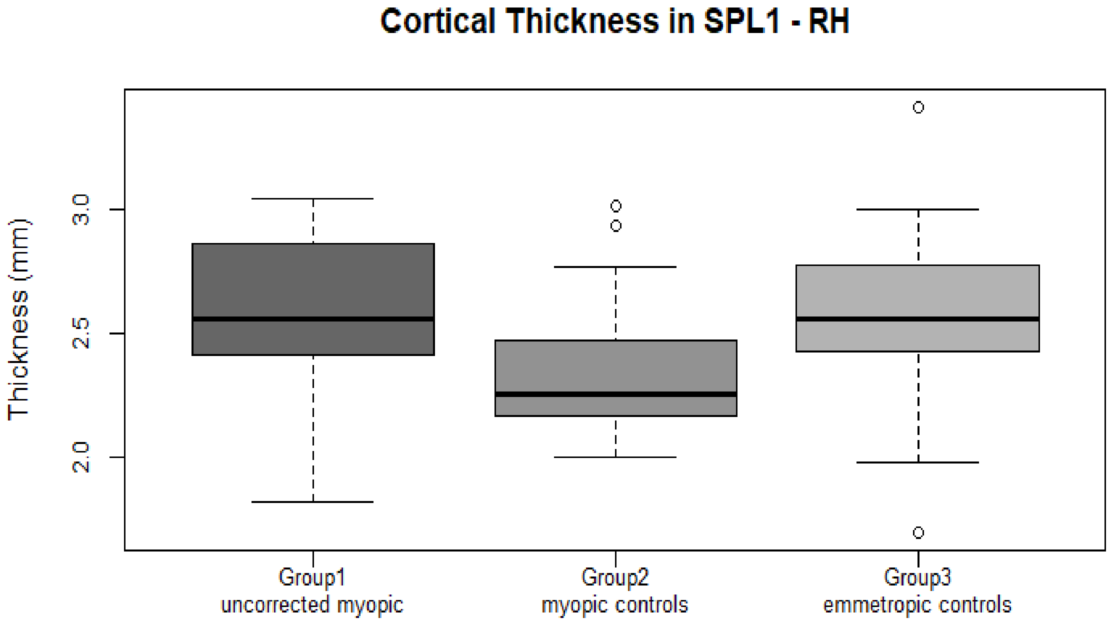

Figure 14: Boxplot for cortical thickness in right SPL1. Differences in cortical thickness between the three experimental groups in SPL1 in the right hemisphere in millimeters (mm). Group 1: uncorrected myopic, Group 2: corrected myopic control group, Group 3: emmetropic.

However, according to our hypothesis, the effect we were looking for should be present when comparing Group 1 against the other two groups but should not be present when comparing Group 2 and Group 3. Since this is not the case for this ROI, the difference in cortical thickness might be due to other factors.

Another region that showed significant differences was the ROI aIPS in the right hemisphere only.

The one-way ANOVA in this ROI showed an adjusted significance of $p=0.012$ and a medium effect size $\eta^2=0.14$ (Cohen, 1992). The posthoc pairwise T-Tests showed a significantly thicker cortex in this region between Group 1 and Group 3 and a large effect (t-test, $p=0.009$, $d=0.83$) (Cohen, 1988). The difference between Group 1 and Group 2 was not significant and showed a small effect (t-test, $p=0.239$, $d=0.37$). The difference between Group 2 and Group 3 was also non-significant with a small effect (t-test, $p=0.668$, $d= 0.45$) (Figure 15). This shows that we can reject the null hypothesis about the absence of group differences.

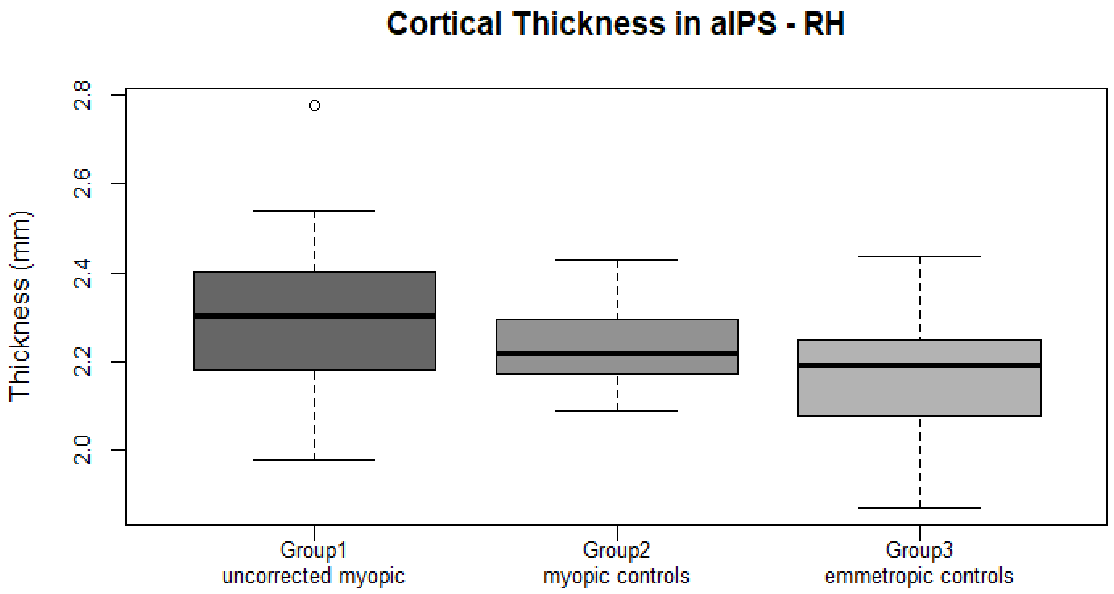

Figure 15: Boxplot for cortical thickness in right aIPS. Differences in cortical thickness between the three experimental groups in aIPS in the right hemisphere in millimeters (mm). Group 1: uncorrected myopic, Group 2: corrected myopic control group, Group 3: emmetropic.

In accordance with our hypothesis, we tested whether Group 1 showed an increased cortical thickness in this ROI when compared to the other two groups. To accomplish that we investigated the group effect in combining the control groups 2 and 3 into one group and comparing it against Group 1. Here, the medium significant effect was still present (t-test, p=0.022, d=0.78).

Table 3 lists the average cortical thickness in ROIs that showed significant differences in cortical thickness between groups.

Average Cortical Thickness in significant ROIs (mm)		
	SPL1 RH	aIPS RH
Group 1	2.605	2.319
Group 2	2.355	2.233
Group 3	2.548	2.176

Table 3: Average cortical thickness in significant ROIs. Thickness in mm in SPL1 and aIPS in the right hemisphere for each experimental group.

ANOVA and Kruskal-Wallis Test showed no significant differences in any of the ROIs in the left hemisphere (Table 4).

	Results of ANOVA and Kruskal-Wallis Test for each ROI and Hemisphere				
	Left ROIs	F-Value/Chi²	P-Value	effect size η^2	Test
Left Hemisphere	V1	0.097	0.908	0.003	ANOVA
	V2	0.098	0.907	0.003	ANOVA
	V3	0.418	0.660	0.01	ANOVA
	IPS0	1.071	0.350	0.04	ANOVA
	IPS1	0.958	0.390	0.03	ANOVA
	IPS2	0.367	0.694	0.01	ANOVA
	IPS3	0.167	0.847	0.01	ANOVA
	IPS4	0.934	0.939	0.03	KWT
	IPS5	0.434	0.650	0.02	ANOVA
	SPL1	0.323	0.725	0.01	ANOVA
	SPL0	0.613	0.545	0.02	ANOVA
	aIPS	0.100	0.905	0.003	ANOVA
	evisual	1.000	0.374	0.03	ANOVA
	Right ROIs	F-Value/Chi²	P-Value	effect size η^2	Test
Right Hemisphere	V1	0.498	0.610	0.02	ANOVA
	V2	0.859	0.429	0.03	ANOVA
	V3	1.313	0.277	0.04	ANOVA
	IPS0	1.193	0.551	0.01	KWT
	IPS1	1.422	0.491	0.01	KWT
	IPS2	1.854	0.166	0.06	ANOVA
	IPS3	4.040	0.133	0.04	KWT
	IPS4	0.766	0.470	0.03	ANOVA
	IPS5	1.110	0.337	0.04	ANOVA
	SPL1*	7.811	0.020	0.10	KWT
	SPL0	1.139	0.327	0.04	ANOVA
	aIPS*	4.768	0.012	0.14	ANOVA
	evisual	0.115	0.892	0.004	ANOVA

Table 4: Statistical analysis of the differences between groups. Analysis performed using ANOVA and Kruskal-Wallis test for all ROIs in each hemisphere. Significant results marked with an asterisk (*).

4.4. Regression Analysis

For the regression analysis with the visual acuity score on the Freiburg Visual Acuity and Contrast Test as predictor of the cortical thickness we found several points on the cortex that seem to correlate with the visual acuity (Figure 16). Although none of these regions survived the multiple comparison correction, the peak in the right anterior part of the IPS in the regression seems to correspond with the peak in the group comparison analysis using the ANOVA, and partially overlaps with the aIPS ROI. The convergence of the regression and group comparison results in the right aIPS suggest that the lack of difference between Group 1 and Group 2 in this region may be due to the fact that self-report of visual acuity may have been a suboptimal criterion for group assignment. Our objective laboratory test of visual acuity clearly predicts cortical thickness in the aIPS.

Participant’s age, which was added as a covariate, did not significantly predict cortical thickness in any of the cortical regions.

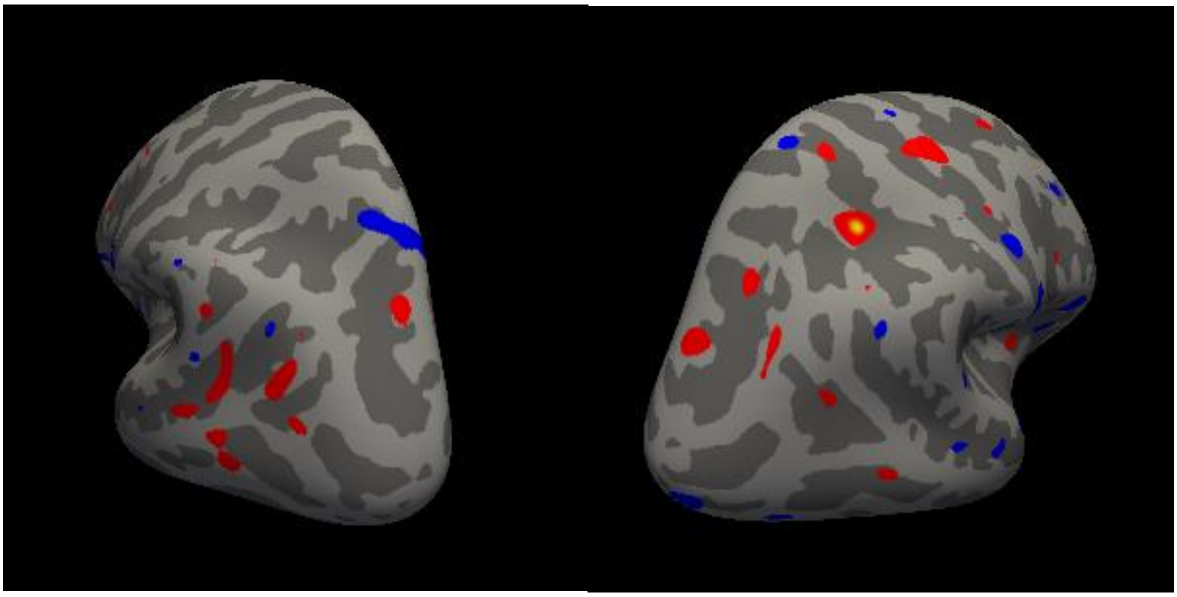

Figure 16: Averaged significance map for regression of cortical thickness and visual acuity. Displayed for the right (on the right) and the left hemisphere (on the left) showing cortical regions where thickness significantly correlates with visual acuity. Red shows positive correlation where blue spots show negative correlation.

We found a significant effect of gender, which was added as another covariate, in the caudal middle frontal region of the left cortex hemisphere where the correlation survived multiple comparison correction (Figure 17). However, this effect of gender is unrelated to our hypothesis and is therefore irrelevant for this thesis.

Figure 17: Lateral view of the left cortical hemisphere. The cortical region where thickness and gender seem to correlate, here marked purple.

5. Discussion

The guiding research question for this thesis was whether decreased visual acuity in subjects with uncorrected myopia is accompanied by changes in cortical thickness. We hypothesized that cortical thickness in the parietal cortex will be increased in subjects with uncorrected myopia in comparison to the two control groups. We further hypothesized that the thickness in the occipital cortex will not show any differences in the uncorrected myopia group when compared to subjects with normal visual acuity, since we expected the effects of top-down and bottom-up changes due to unreliable visual input in perception to cancel out.

In this study, we examined the cortical thickness of participants with uncorrected myopia in predefined regions of interest associated with visual perception. The thickness was then compared to a myopic and an emmetropic control group. The findings suggest that there might be differences in cortical thickness in this population. Two regions of interest, namely aIPS which is located in the anterior intraparietal sulcus, and SPL1 which can be found in the superior parietal lobe showed significant differences between the three groups. Especially the findings in aIPS support our hypothesis. Additionally, the whole-brain analysis revealed multiple clusters throughout the cortex in which the uncorrected myopia group differed in mean cortical thickness from the other two groups. However, these findings did not survive the correction for multiple comparisons.

5.1. Region-of-interest Results

5.1.1. Anterior Intraparietal Sulcus

The only ROI that showed a significant difference in cortical thickness when comparing the uncorrected myopia group (Group 1) against the other two control groups was aIPS in the right hemisphere, which is located in the right anterior intraparietal sulcus.

Group 1 showed a significantly thicker aIPS when compared to emmetropic controls. When comparing Group 1 with myopic controls, mean aIPS thickness was still higher in Group 1, however, the difference failed to reach significance. The two control groups did not differ significantly in thickness. When investigating the group effect, Group 1 still showed a significantly thicker aIPS than the other two groups combined.

In their fMRI study, Zaretskaya and collaborators (2013) found that activity in aIPS correlated with the perception of grouped illusory Gestalt images. When interfering with the activity in aIPS with transcranial magnetic stimulation, the emerging Gestalt percept was perceived for a significantly shorter period. This suggests that aIPS is involved in the perceptual binding of elements into Gestalt shapes (Zaretskaya et al., 2013). PET studies in healthy persons showed the involvement of aIPS regions in tactile and visual shape processing as well as the processing of 3D structures (Grefkes & Fink, 2005). In the macaque cortex, the neurons in the region equivalent to aIPS in humans showed strong responses to size, shape, and orientation of objects (Grefkes & Fink, 2005).

Furthermore, the findings of Ruff and colleagues (2009) and Zaretskaya and colleagues (2013) demonstrated that activity in aIPS modulates activity in primary visual areas. This is consistent with studies that reported deactivation in V1 during shape perception (Murray et al., 2002) and predictable motion (Alink et al., 2010).

AIPS has been associated not only with grouping, but also with spatial attention and perceptual selection (Corbetta & Shulman, 2002; Yantis & Serences, 2003). However, Romei and collaborators (2011) suggest a role of aIPS in attention control in Gestalt perception by mediating between local and global stimulus aspects. Consistent with these findings, Qiu and collaborators (2007) suggest a link between attentional selection and perceptual grouping.

Additionally, Geng & Mangun (2009) indicate in their study that aIPS plays a role in visual attention driven by salient bottom-up influences rather than goal-directed attention which would not support the predictive coding approach.

Following our hypotheses, uncorrected myopia results in blurry visual input, which makes more guesswork necessary to compensate for the lack of precise information in the visual input. This can require the individual to actively combine perceived contours in order to create meaningful content, thus increasing the workload on the cortical areas involved in object and shape perception and recognition. In the context of PP theories, this would suggest aIPS region as a candidate for a higher-level processing region that can modulate the lower hierarchical levels by passing down predictions. Hence, the increased thickness in aIPS in low visual acuity can be used as supporting evidence for our hypothesis.

5.1.2. Superior Parietal Lobe

The second ROI that showed significant differences between groups is the region SPL1 on the right hemisphere. The results of the MRI scanning showed a significantly lower cortical thickness in this region in the myopic control group (Group 2) when compared to the uncorrected myopia group (Group 1). Group 2 also showed decreased thickness in SPL1 when compared to emmetropic controls (Group 3), however, this difference did not reach significance. The small difference between the slightly thicker cortex in Group 1 and Group 3 can be considered neglectable. The ROI SPL1 extends from the intersection of intraparietal and postcentral sulcus into the superior parietal lobule and has been found to be involved in the execution of saccadic eye movements (Konen & Kastner, 2008).

One possible explanation for this effect is that spectacle wearers tend to execute fewer explorative saccades since the lenses used in the spectacles possess one optimal vision point at the very center of the lens. Eye movement results in a different distance and various angles between the pupil and the center of the lens and this results in altered refractive properties with consecutive reduced visual acuity for the spectacle wearer (Grehn, 2019). These findings suggest that the difference in cortical thickness in myopic individuals may be influenced not only by low visual acuity but also by other factors such as oculomotor behavior.

5.2. Whole-brain Results

Whole-brain analysis of the cortical thickness did not show any significant differences between the experimental Group 1 and the other two groups after multiple comparison correction.

However, the results we obtained before correcting for multiple comparisons show numerous clusters throughout the entire cortex. What is striking is that there are more clusters on the right hemisphere than there are on the left hemisphere.

This result fits well with the known right hemisphere specialization for perceptual functions. Corballis (2003) stated that studies on split-brain patients revealed that the right hemisphere might be more involved in visual tasks than the left counterpart. The right hemisphere outperformed the left in spatial discrimination tasks like detecting small differences in line orientation. Corballis concluded that the left hemisphere may process visual stimuli preferentially for identity information, at the expense of spatial precision and that the right hemisphere can be conceived as more perceptually intelligent than the left. Additionally, when looking at illusory contour images, the right hemisphere was considerably better in perceiving a Gestalt (Corballis, 2003).

Supporting experimental evidence for role of the right hemisphere in perception comes from Jalal and colleagues (2021), who claim the right hemisphere plays an important role in attentional orienting and that new sensory information is first computed in the right hemisphere, facilitating the detection of the bigger picture, like a Gestalt. This allows exploring the visual field for novel patterns. This is also true in the animal kingdom (Jalal, 2021; McGilchrist, 2019). Additionally, Engvig and collaborators (2010) showed similar findings, as the memory training led to an increase in cortical thickness predominantly in the right hemisphere, which they related to the task requirement of sustaining attention and visuospatial processing.

Altogether, the fact that most clusters concentrate in the right hemisphere seems to indicate that reduced visual acuity might affect the perceptual function and its morphometric correlates.

5.2.1. Notable Clusters in Whole-Brain Analysis

Although none of the clusters survived the correction for multiple comparisons, their location demonstrates spatial specificity to regions involved in the visual and multimodal perceptual function. The most noteworthy clusters detected during whole-brain analysis comprise several regions discussed in more detail below.

There is a significant cluster of increased cortical thickness in the middle temporal area in both hemispheres, although the cluster is bigger in the right hemisphere. With regard to function, this region is well-known to be involved in visual processing, shows retinotopic organization, and contains a high number of motion-sensitive neurons (Bear et al., 2020; Kolster et al., 2010).

The right inferior parietal region showed another strong cluster. This region is involved in several different processes and functional networks and seems to integrate cross-modal information to ensure comprehension, manipulation, and orientation. The inferior parietal region is involved in speech and articulation, auditory short-term memory, and tactile reception. The caudal part is related to spatial attention, spatial perception, spatial memory, and visuomotor integration (Binkofski et al., 2016).

Lastly, there are clusters in the right superior parietal region which is known to be linked with the occipital lobe and is involved with aspects of visuospatial perception (Johns, 2014; Stoeckel et al., 2009). The fact that uncorrected clusters coincide with areas known to be involved in visual perception, attention, and multimodal integration suggests that they may not be mere false positives and may become significant after multiple comparison corrections in a larger sample or a sample with stronger myopia effects.

5.3. Regression Analysis

The second approach to investigate the relationship of low visual acuity and cortical thickness involved regression analysis over the whole sample with measured visual acuity as a predictor. This was done for all 13 ROIs, respectively to examine whether these two variables are linked and additionally to control for non-perfect group assignment. However, the regression analysis for cortical thickness and visual acuity showed no significant outcome. This could be accounted for by the relatively good visual far acuity in all three groups due to the low degree of myopia in most of Group 1.

Since biological age is known to affect cortical thickness, the regression analysis for cortical thickness included age as a possible covariate. (Thambisetty et al., 2010). Yet, these findings did not show any significant results either, suggesting that the age distribution in our sample was too small to influence the cortical thicknesses.

5.4. Theoretical Framework

In our study, we found some evidence in support of a stronger role of top-down processes in visual perception in low visual acuity within the predictive processing framework. We found increased cortical thickness in the region of the right anterior intraparietal sulcus which could function as a source of predictions. However, this is the only ROI we found in the experiment that shows significant differences between the experimental group and the two control groups. This circumstance could be due to the small sample size; however, it requires us to critically evaluate the underlying hypothesis that unreliable visual input, caused by low visual acuity, results in a stronger role of top-down predictions in perception.

Predictive processing theory enjoys increasing attention as a unifying principle in cognition, action, and perception, yet, there is also a lot of criticism. Critics argue that PP is too vague to be used as an explanation for cognitive processes, not least because of the fact that the neural circuits that underlie predictive coding are still speculative and fail to be empirically confirmed (Litwin & Miłkowski, 2020).

Apart from missing experimental evidence for predictive processing, there is evidence that blurry visual input does not necessarily lead to an impairment of visual perception. Sabesan & Yoon (2010) suggest neural compensatory mechanisms on a chemical level that increase visual acuity in subjects with refraction error due to corneal disorders by adapting to the blur and hence decreasing the noise of the visual input in the visual system. Mechanisms like that could also be present in refractive errors due to myopia, creating new ‘rules’ for interpretation of the unclear visual input rejecting the need for a clear retinal image in perception.

Similar evidence comes from Rossi and collaborators (2007) who found that subjects with lower myopia performed worse in visual acuity testing than emmetropes even when their myopia was fully compensated. The authors suggest neural and/or retinal factors limit the visual acuity in low myopes adaption mechanisms to the blurry visual input. This is in accordance with other blur adaption studies that show cortical adaptions to blurry visual input after exposure to blur during extended periods of time (Cufflin & Mallen, 2020; George & Rosenfield, 2004; Poulere et al., 2013). These findings shed a different light on the concept of subjective visual acuity as well as the measurement of which and raise the question of whether myopes really perceive their environment as blurry as presumed. Although these findings do not rule out top-down processes as a possible source of these adaptions, it raises questions about the dominance of top-down influences in low visual acuity since bottom-up influences seem to shape visual perception and visual acuity on a neural level, increasing the interpretability of the blurry input.

Nevertheless, there is also lots of support for our hypothesis and the increased role of top-down processes. Yon & Firth (2021), who introduce an alternative perspective in terms of precision weighing. They argue that the perceptual system combines different signals according to their reliability or uncertainty. Agents achieve this by (subconsciously) acknowledging the noise and variance in the sensory input and considering the volatility of the environment. According to their reasoning, prediction errors are weighted according to their reliability and the agent's uncertainty. Hence, in a less reliable environment, which is harder to predict, top-down predictions guide visual perception and in a reliable environment, perception should be dominated by bottom-up input. Additionally, the agent's (subconscious) certainty or uncertainty about the environment plays into the weighing of the prediction. Certainty leads to more reliable and less imprecise predictions and possible prediction errors are weighed higher. In contrast, when we are aware that the environment is volatile, we weigh prediction errors less, since our beliefs are poor predictors, and the sensory information contains a lot of non-informative noise. Complementarily, Kok (2015) states that perceptual inference must take the reliability of sensory information (precision) into account in order to function efficiently. This implies that sensory information weighs more when it has high precision. When sensory signals are ambiguous and low in precision they should be weighted less and top-down predictions should guide perception. There is discussion whether attention is the process that guides precision in perception. This process of modulating weights during the perceptual process is thought to be facilitated by neuromodulators (Lawson et al., 2021).

It follows, that if the agent is uncertain, meaning he or she is aware of his or her myopia and low visual acuity, cognizant about the unreliability of his or her visual input, and considers the sensory information not particularly trustworthy, top-down predictions guide the perceptual process. Prediction errors are not weighed as strongly if the myopic agent is aware of the low reliability of the visual input.

To subjectively monitor the reliability of our own mind is at the core of high-level cognitive abilities like metacognition. This reliability is the basis of certainty and uncertainty and the feeling of confidence in our own decisions (Yon & Frith, 2021). Growing evidence suggests that the feeling of confidence is influenced by mechanisms that track the precision of other representations. In a study, Geurts and collaborators (2021) recorded the brain activity of participants while they made perceptual judgments about tilted visual patterns, recording explicit confidence ratings about their choices. They found that the measure of neural precision was able to predict the participants' confidence rating on that trial. It may therefore be important in future studies to consider not only the objective visual acuity of individuals but also their metacognitive subjective estimate of the reliability of if their own perceptual input.

To summarize, according to the results of this study, it is not possible to give a definite answer to the research question of whether decreased visual acuity in subjects with uncorrected myopia is accompanied by changes in cortical thickness.

In support of our research question, we found one region (aIPS) in the parietal cortex where the uncorrected myopia group showed higher mean thickness values than the control groups. Although the difference between Group 1 and Group 2 failed to reach significance, there was still a trend toward higher values in Group 1. The findings in SPL1 are likely due to something other than low visual acuity since the effect that was present when comparing Group1 and Group 2 was far from significant between Group 1 and Group 3. Whole-brain analysis showed multiple significant clusters in cortical regions known to be involved in visual processing, however, none of these clusters survived the correction for multiple comparisons. These findings can be interpreted in support of our hypothesis; however, the lack of significance could be attributed to the small sample size.

As for findings in the occipital lobe, we did not find any significant differences in cortical thickness values or noteworthy trends in thickness in the early visual areas V1-V3.

5.5. Limitations

The study shows several limitations, the most significant being the participant sample. The visual acuity test, which was performed after the scanning, showed a significantly decreased visual acuity in the experimental group (Group 1) in comparison with the myopic controls (Group 2) and emmetropic controls (Group 3). However, median myopia in Group 1 was very small with only 0.05 dpt for the left and the right eye. Accordingly, the visual acuity in this group was only minimally below normal visual acuity (0.07 logMAR for the right eye and 0.03 logMAR for the left eye) and for binocular acuity, it was even slightly better than what is considered normal visual acuity (-0.07 logMAR). The visual far point for myopia that small is for otherwise healthy eyes at about 2 m distance. In modern urban environments, and especially in academic life, most visual demands are under 2 m distance from the eye. Reading and working on computer screens and mobile devices happens mostly within the distance of 2 m, which leaves plenty of clear visual input for the myopic Group 1 in their everyday life. This is especially true for the participants of this study, which were all under 36 years of age and the majority (80%) were students. This circumstance is very relevant for this study and could be compensated in future studies by a higher degree of myopia in the participants in Group 1, or, alternatively, a bigger sample that would have more statistical power for such small visual acuity effects.

Of course, participants with higher myopia are less likely to turn down optical correction in their day-to-day life, hence suitable participants are harder to find. This would call for collaboration with local ophthalmologists to recruit an effective sample.

Additionally, the separation into the three experimental groups was not always perfect, with participants who initially identified as emmetropic discovering in the course of the visual testing that their visual acuity was decreased below the level expected from a healthy emmetropic eye, which led to the assumption that mild myopia was present in these participants. However, regression analysis of visual acuity and cortical thickness would have revealed a significant correlation that would have compensated for the flawed group assignment. Yet, regression analysis on these variables showed no significant results. Again, this possibly roots in the rather good visual acuity in the uncorrected myopia group and/or the small sample size.

The size of the sample in this study poses considerable limitations on the evaluation of the data. The small amount of data available caused the non-normal distribution of participants' data in multiple instances. This in turn led to the use of non-parametric tests in the statistical analysis of the MRI data, specifically the Kruskal-Wallis Test and Wilcoxon test. Non-parametric tests typically show slower convergence towards the statistical distribution than parametric tests do which is relevant for smaller sample sizes. (Chan & Walmsley, 1997; Imam et al., 2014). Although the exact definition of 'small' in this context varies, this should be considered when interpreting the results.

The small sample size also decreased the statistical power in this study as posthoc power analysis revealed. Low statistical power comes with a variety of problems concerning the validity and credibility of the study. Low statistical power reduces the chance to detect a true effect that holds for the entire population, but also it reduces the likelihood that significant results in the study reflect an actual true effect (Button et al., 2013).

Finally, when interpreting these findings, one needs to be aware of the correlational character of this study. Hence, the study design does not allow to draw conclusions about the nature of the relationship the two variables, cortical thickness, and uncorrected myopia have.

5.6. Further Research – Outlook

This experiment clearly calls for multiple extensions and follow-ups. First, more data is needed to increase the statistical power of observed effects. Continuing the experiment to increase the sample size could give rise to more significant and more meaningful findings. Alternatively, a higher degree of myopia in Group 1 might increase the effect size and also yield more significant findings.

Second, to investigate the role of cortical thickness within the framework of predictive processing theories it would be crucial to investigate the individual thickness of different cortical layers. As pointed out by Shipp (2016), different cortical layers play different roles in the predictive coding circuit. The resolution of the 3-Tesla MRI Siemens Magnetom Vida scanner that was used in this experiment poses a limiting factor on the informative value of the findings in this study. The resolution does not allow to measure the thickness in individual cortical layers that would allow to draw conclusions about the demand in individual layers. While functional MRI studies across cortical layers are becoming more and more popular with the increasing availability of ultra-high field MRI (Han et al., 2021; Shao et al., 2021; Zaretskaya, 2021) morphometric changes across the cortical layers have not been so extensively investigated. This could be an interesting avenue for future research.

Finally, a question that remains open and calls for further research is the causal relationship between decreased visual acuity and cortical thickness in the visual cortex or the parietal cortex. A potential setup to study possible causal relationships between these variables involves a within-subject design with suitable probands before and after refractive surgery or operation of acquired juvenile cataracts.

6. Conclusion

Myopia causes low visual far acuity, however, some people with myopia decide to accept this circumstance to avoid having to wear spectacles throughout the day. This population frequently faces blurry and unreliable visual input, hence must deal with high noise in their bottom-up input. Accordingly, to manage their everyday life, uncorrected myopes need to rely more strongly on top-down processes in visual perception. Within the framework of predictive processing theories, this implies increased workload on higher cortical regions involved in the generation of top-down predictions as well as a decreased role of lower visual areas.

The thickness of the neocortex is known to vary, depending on the cognitive demand. This thesis makes use of this circumstance by examining whether decreased visual acuity in probands with uncorrected myopia is related to changes in cortical thickness.

An experiment was conducted using MRI to examine the difference in cortical thickness in 13 regions of interest between three experimental groups. The experimental group comprised 19 subjects with uncorrected myopia, the second group was a myopic control group which consisted of 18 myopic subjects who wore their optical correction frequently and reported good visual acuity with it. The last group was an emmetropic control group with 23 participants who also reported good visual acuity without any optical correction.

We hypothesized that due to increased workload in the higher visual areas the regions concerned with visual perception in the parietal cortex will be increased in the uncorrected myopia group in comparison to the two control groups. For the occipital cortex, we expected no change in cortical thickness due to cancelling out effects of less bottom-up perception and stronger top-down input in this region.

The results for whole-brain analysis showed multiple significant clusters throughout the entire cortex, the majority of clusters showing in the right hemisphere in regions known to play a role in visual processing. However, none of these regions survived correction for multiple comparisons.

As for ROI analysis, two regions of interest in the parietal cortex showed significant effects. One region in the anterior part of the intraparietal sulcus showed to be significantly thicker in the uncorrected myopia group when compared to the other two control groups. This region is known to play a role in higher-order visual processing, which would be in line with our hypothesis. Also, one region on the superior parietal lobe was found to be significantly thinner in the fully corrected myopic control group in comparison with the uncorrected myopic group and emmetropic controls, although it did not reach significance in comparison with the emmetropes. This finding might be related to factors other than visual acuity since the uncorrected myopia group and the emmetropic controls did not differ significantly. One possible explanation could be decreased oculomotor behavior due to eye-glasses with centralized focus.

Regression analysis of cortical thickness and the visual acuity score found in prior testing showed no significant correlation between these two variables. No significant differences in the primary visual areas (V1-V3) between the three groups were detected.

The findings suggest that there might be a correlation between visual acuity and thickness in certain cortical regions, however, the study did not yield enough statistical power to reach significance in most instances. The parietal cortex region showed to be significantly thicker in the region of the right anterior parietal sulcus in the uncorrected myopes when compared to the control groups. The occipital cortex showed no significant differences in cortical thickness between the three groups and no noteworthy trends in thickness that failed to reach significance. Yet, the findings in the occipital cortex could be due to the small sample size.

Overall, the aim of this thesis, which was to conduct an MRI experiment to answer the research question of whether decreased visual acuity in subjects with uncorrected myopia is related to changes in the cortical thickness, was met. The findings suggest increased cortical thickness in regions that could serve as sources for top-down predictions which would be in line with assumptions underlying predictive processing theory.

Nevertheless, inferring causality should be done with caution since the study faces limitations, most significantly the small sample size and the low degree of myopia in the uncorrected myopia group. This study would benefit from an extension of the participant sample to increase statistical power. Also, there is the need for follow-up studies to investigate the relationship between visual acuity and cortical thickness more closely.

7. References

Adesnik, H., & Naka, A. (2018). Cracking the Function of Layers in the Sensory Cortex. Neuron, 100(5), 1028–1043. https://doi.org/10.1016/j.neuron.2018.10.032

Alink, A., Schwiedrzik, C. M., Kohler, A., Singer, W., & Muckli, L. (2010). Stimulus Predictability Reduces Responses in Primary Visual Cortex. Journal of Neuroscience, 30(8), 2960–2966. https://doi.org/10.1523/JNEUROSCI.3730-10.2010

Anzai, A., Peng, X., & Van Essen, D. C. (2007). Neurons in monkey visual area V2 encode combinations of orientations. Nature Neuroscience, 10(10), 1313–1321. https://doi.org/10.1038/nn1975

Ayzenberg, V., Kamps, F. S., Dilks, D. D., & Lourenco, S. F. (2022). Skeletal representations of shape in the human visual cortex. Neuropsychologia, 164, 108092. https://doi.org/10.1016/j.neuropsychologia.2021.108092

Bach, M. (1996). The Freiburg Visual Acuity test—Automatic measurement of visual acuity. Optometry and Vision Science, 73(1), 49–53. https://doi.org/10.1097/00006324-199601000-00008

Baird, P. N., Saw, S.-M., Lanca, C., Guggenheim, J. A., Smith III, E. L., Zhou, X., Matsui, K.-O., Wu, P.-C., Sankaridurg, P., Chia, A., Rosman, M., Lamoureux, E. L., Man, R., & He, M. (2020). Myopia. Nature Reviews Disease Primers, 6(1), 99. https://doi.org/10.1038/s41572-020-00231-4

Baroncelli, L., & Lunghi, C. (2021). Neuroplasticity of the visual cortex: In sickness and in health. Experimental Neurology, 335, 113515. https://doi.org/10.1016/j.expneurol.2020.113515

Bear, M. F., Connors, B. W., & Paradiso, M. A. (2020). Neuroscience: Exploring the brain (Enhanced fourth edition). Jones & Bartlett Learning.

Binkofski, F. C., Klann, J., & Caspers, S. (2016). Chapter 4—On the Neuroanatomy and Functional Role of the Inferior Parietal Lobule and Intraparietal Sulcus. In G. Hickok & S. L. Small (Eds.), Neurobiology of Language (pp. 35–47). Academic Press.

Blasdel, G., & Fitzpatrick, D. (1984). Physiological organization of layer 4 in macaque striate cortex. The Journal of Neuroscience, 4(3), 880–895. https://doi.org/10.1523/JNEUROSCI.04-03-00880.1984

Braddick, O. J., O'Brien, J. M. D., Wattam-Bell, J., Atkinson, J., Hartley, T., & Turner, R. (2001). Brain Areas Sensitive to Coherent Visual Motion. Perception, 30(1), 61–72. https://doi.org/10.1068/p3048

Brainard, D. H. (2009). Bayesian Approaches to Color Vision. In M. S. Gazzaniga (Ed.), The cognitive neurosciences (4th ed, pp. 395–408). MIT Press.

Burge, W. K., Griffis, J. C., Nenert, R., Elkhetali, A., DeCarlo, D. K., ver Hoef, L. W., Ross, L. A., & Visscher, K. M. (2016). Cortical thickness in human V1 associated with central vision loss. Scientific Reports, 6(1), 23268. https://doi.org/10.1038/srep23268

Burnett-Zeigler, I., Walton, M. A., Ilgen, M., Barry, K. L., Chermack, S. T., Zucker, R. A., Zimmerman, M. A., Booth, B. M., & Blow, F. C. (2012). Prevalence and Correlates of Mental Health Problems and Treatment Among Adolescents Seen in Primary Care. Journal of Adolescent Health, 50(6), 559–564. https://doi.org/10.1016/j.jadohealth.2011.10.005

Button, K. S., Ioannidis, J. P. A., Mokrysz, C., Nosek, B. A., Flint, J., Robinson, E. S. J., & Munafò, M. R. (2013). Power failure: Why small sample size undermines the reliability of neuroscience. Nature Reviews Neuroscience, 14(5), 365–376. https://doi.org/10.1038/nrn3475

Castaldi, E., Lunghi, C., & Morrone, M. C. (2020). Neuroplasticity in adult human visual cortex. Neuroscience & Biobehavioral Reviews, 112, 542–552. https://doi.org/10.1016/j.neubiorev.2020.02.028

Chan, Y., & Walmsley, R. P. (1997). Learning and Understanding the Kruskal-Wallis One-Way Analysis-of-Variance-by-Ranks Test for Differences Among Three or More Independent Groups. Physical Therapy, 77(12), 1755–1761. https://doi.org/10.1093/ptj/77.12.1755

Clark, A. (2013). Whatever next? Predictive brains, situated agents, and the future of cognitive science. Behavioral and Brain Sciences, 36(3), 181–204. https://doi.org/10.1017/S0140525X12000477

Cohen, J. (1988). Statistical Power Analysis for the Behavioral Sciences (0 ed.). Routledge. https://doi.org/10.4324/9780203771587

Cohen, J. (1992). A power primer. Psychological Bulletin, 112(1), 155–159. https://doi.org/10.1037/0033-2909.112.1.155

Colenbrandner, A. (1989). Measuring Vision and Vision Loss. In W. Tasman & G. W. Weinstein (Eds.), Duane's clinical ophthalmology. Vol. 5: [Ophthalmic surgery] / Sect. Ed.: George W. Weinstein (Rev. ed, Vol. 5). Lippincott.

Cooper, J., & Tkatchenko, A. V. (2018). A Review of Current Concepts of the Etiology and Treatment of Myopia. Eye & Contact Lens: Science & Clinical Practice, 44(4), 231–247. https://doi.org/10.1097/ICL.0000000000000499

Corballis, P. M. (2003). Visuospatial processing and the right-hemisphere interpreter. Brain and Cognition, 53(2), 171–176. https://doi.org/10.1016/S0278-2626(03)00103-9

Corbetta, M., & Shulman, G. L. (2002). Control of goal-directed and stimulus-driven attention in the brain. Nature Reviews Neuroscience, 3(3), 201–215. https://doi.org/10.1038/nrn755

Cufflin, M. P., & Mallen, E. A. (2020). Blur adaptation: Clinical and refractive considerations. Clinical and Experimental Optometry, 103(1), 104–111. https://doi.org/10.1111/cxo.13033

Dale, A. M., Fischl, B., & Sereno, M. I. (1999). Cortical Surface-Based Analysis. NeuroImage, 9(2), 179–194. https://doi.org/10.1006/nimg.1998.0395

Demb, J. B., & Singer, J. H. (2015). Functional Circuitry of the Retina. Annual Review of Vision Science, 1(1), 263–289. https://doi.org/10.1146/annurev-vision-082114-035334

den Ouden, H. E. M., Friston, K. J., Daw, N. D., McIntosh, A. R., & Stephan, K. E. (2009). A Dual Role for Prediction Error in Associative Learning. Cerebral Cortex, 19(5), 1175–1185. https://doi.org/10.1093/cercor/bhn161

Dougherty, K., Schmid, M. C., & Maier, A. (2019). Binocular response modulation in the lateral geniculate nucleus. Journal of Comparative Neurology, 527(3), 522–534. https://doi.org/10.1002/cne.24417

Dumoulin, S. O., Harvey, B. M., Fracasso, A., Zuiderbaan, W., Luijten, P. R., Wandell, B. A., & Petridou, N. (2017). In vivo evidence of functional and anatomical stripe-based subdivisions in human V2 and V3. Scientific Reports, 7(1), 733. https://doi.org/10.1038/s41598-017-00634-6

Engvig, A., Fjell, A. M., Westlye, L. T., Moberget, T., Sundseth, Ø., Larsen, V. A., & Walhovd, K. B. (2010). Effects of memory training on cortical thickness in the elderly. NeuroImage, 52(4), 1667–1676. https://doi.org/10.1016/j.neuroimage.2010.05.041

Ernst, M. O., & Banks, M. S. (2002). Humans integrate visual and haptic information in a statistically optimal fashion. Nature, 415(6870), 429–433. https://doi.org/10.1038/415429a

Feldman, H., & Friston, K. J. (2010). Attention, Uncertainty, and Free-Energy. Frontiers in Human Neuroscience, 4. https://doi.org/10.3389/fnhum.2010.00215

Fischl, B., & Dale, A. M. (2000). Measuring the thickness of the human cerebral cortex from magnetic resonance images. Proceedings of the National Academy of Sciences, 97(20), 11050–11055. https://doi.org/10.1073/pnas.200033797

Fjell, A. M., Westlye, L. T., Grydeland, H., Amlien, I., Espeseth, T., Reinvang, I., Raz, N., Dale, A. M., Walhovd, K. B., & for the Alzheimer Disease Neuroimaging Initiative. (2014). Accelerating Cortical Thinning: Unique to Dementia or Universal in Aging? Cerebral Cortex, 24(4), 919–934. https://doi.org/10.1093/cercor/bhs379

FreeSurfer, T. (2021). Freesurfer Software (6.0.1) [Computer software]. FreeSurfer. https://surfer.nmr.mgh.harvard.edu/

Freitas, C., Perez, J., Knobel, M., Tormos, J. M., Oberman, L., Eldaief, M., Bashir, S., Vernet, M., Peña-Gómez, C., & Pascual-Leone, A. (2011). Changes in Cortical Plasticity Across the Lifespan. Frontiers in Aging Neuroscience, 3. https://doi.org/10.3389/fnagi.2011.00005

Friston, K. (2008). Hierarchical Models in the Brain. PLoS Computational Biology, 4(11), e1000211. https://doi.org/10.1371/journal.pcbi.1000211

Friston, K. (2010). The free-energy principle: A unified brain theory? Nature Reviews Neuroscience, 11(2), 127–138. https://doi.org/10.1038/nrn2787

Frolov, A., Feuerstein, J., & Subramanian, P. S. (2017). Homonymous Hemianopia and Vision Restoration Therapy. Neurologic Clinics, 35(1), 29–43. https://doi.org/10.1016/j.ncl.2016.08.010

Garg, A. K., Li, P., Rashid, M. S., & Callaway, E. M. (2019). Color and orientation are jointly coded and spatially organized in primate primary visual cortex. Science, 364(6447), 1275–1279. https://doi.org/10.1126/science.aaw5868

Geng, J. J., & Mangun, G. R. (2009). Anterior Intraparietal Sulcus is Sensitive to Bottom–Up Attention Driven by Stimulus Salience. Journal of Cognitive Neuroscience, 21(8), 1584–1601. https://doi.org/10.1162/jocn.2009.21103

George, S., & Rosenfield, M. (2004). Blur Adaptation and Myopia: Optometry and Vision Science, 81(7), 543–547. https://doi.org/10.1097/00006324-200407000-00016

Geurts, L. S., Cooke, J. R. H., van Bergen, R. S., & Jehee, J. F. M. (2021). Subjective confidence reflects representation of Bayesian probability in cortex [Preprint]. Neuroscience. https://doi.org/10.1101/2021.04.10.439272

Gollisch, T., & Meister, M. (2010). Eye Smarter than Scientists Believed: Neural Computations in Circuits of the Retina. Neuron, 65(2), 150–164. https://doi.org/10.1016/j.neuron.2009.12.009

Gomel, N., Negari, S., Frucht-Pery, J., Wajnsztajn, D., Strassman, E., & Solomon, A. (2018). Predictive factors for efficacy and safety in refractive surgery for myopia. PLOS ONE, 13(12), e0208608. https://doi.org/10.1371/journal.pone.0208608

Gräf, M. (2012). Sehschärfe. In H. Steffen & H. Kaufmann (Eds.), Strabismus. Georg Thieme Verlag KG.

Grassi, P. R., Zaretskaya, N., & Bartels, A. (2016). Parietal cortex mediates perceptual Gestalt grouping independent of stimulus size. NeuroImage, 133, 367–377. https://doi.org/10.1016/j.neuroimage.2016.03.008

Grefkes, C., & Fink, G. R. (2005). REVIEW: The functional organization of the intraparietal sulcus in humans and monkeys: Intraparietal sulcus in monkeys and humans, C. Grefkes and G. R. Fink. Journal of Anatomy, 207(1), 3–17. https://doi.org/10.1111/j.1469-7580.2005.00426.x

Grehn, F. (2019). Refraktionsfehler: Brillen, Kontaktlinsen und refraktive Chirurgie. In Augenheilkunde (pp. 471–495). Springer, Berlin, Heidelberg.

Han, S., Eun, S., Cho, H., Uludağ, K., & Kim, S.-G. (2021). Improvement of sensitivity and specificity for laminar BOLD fMRI with double spin-echo EPI in humans at 7 T. NeuroImage, 241, 118435. https://doi.org/10.1016/j.neuroimage.2021.118435

Heinrich, S., & Hoffmann, M. (2018). Sehschärfe, Kontrastempfindlichkeit, Farbensehen: Gedanken zu psychophysischen Untersuchungen in der Neuroophthalmologie. Klinische Monatsblätter für Augenheilkunde, 235(11), 1212–1217. https://doi.org/10.1055/a-0715-7918

Helmholtz, H. von. (2005). Treatise on physiological optics (J. P. C. Southall, Ed.; Dover ed). Dover Publications.

Holden, B. A., Fricke, T. R., Wilson, D. A., Jong, M., Naidoo, K. S., Sankaridurg, P., Wong, T. Y., Naduvilath, T. J., & Resnikoff, S. (2016). Global Prevalence of Myopia and High Myopia and Temporal Trends from 2000 through 2050. Ophthalmology, 123(5), 1036–1042. https://doi.org/10.1016/j.ophtha.2016.01.006

Hosoya, T., Baccus, S. A., & Meister, M. (2005). Dynamic predictive coding by the retina. Nature, 436(7047), 71–77. https://doi.org/10.1038/nature03689

Hubel, D. H., & Wiesel, T. N. (1962). Receptive fields, binocular interaction and functional architecture in the cat's visual cortex. The Journal of Physiology, 160(1), 106–154. https://doi.org/10.1113/jphysiol.1962.sp006837

Hubel, D. H., & Wiesel, T. N. (1972). Laminar and columnar distribution of geniculo-cortical fibers in the macaque monkey. The Journal of Comparative Neurology, 146(4), 421–450. https://doi.org/10.1002/cne.901460402

Hupé, J. M., James, A. C., Payne, B. R., Lomber, S. G., Girard, P., & Bullier, J. (1998). Cortical feedback improves discrimination between figure and background by V1, V2 and V3 neurons. Nature, 394(6695), 784–787. https://doi.org/10.1038/29537

Imam, A., Mohammed, U., & Moses Abanyam, C. (2014). On Consistency and Limitation of paired t-test, Sign and Wilcoxon Sign Rank Test. IOSR Journal of Mathematics, 10(1), 01–06. https://doi.org/10.9790/5728-10140106

Jalal, B. (2021). "Men Fear Most What They Cannot See." sleep paralysis "Ghost Intruders" and faceless "Shadow-People"—The role of the right hemisphere and economizing nature of vision. Medical Hypotheses, 148, 110521. https://doi.org/10.1016/j.mehy.2021.110521

Jiang, L., Cao, X., Li, T., Tang, Y., Li, W., Wang, J., Chan, R. C., & Li, C. (2016). Cortical Thickness Changes Correlate with Cognition Changes after Cognitive Training: Evidence from a Chinese Community Study. Frontiers in Aging Neuroscience, 8(118). https://doi.org/10.3389/fnagi.2016.00118

Johns, P. (2014). Chapter 3—Functional neuroanatomy. In P. Johns (Ed.), Clinical Neuroscience (pp. 27–47). Churchill Livingstone.

Johnston, J., Seibel, S.-H., Darnet, L. S. A., Renninger, S., Orger, M., & Lagnado, L. (2019). A Retinal Circuit Generating a Dynamic Predictive Code for Oriented Features. Neuron, 102(6), 1211-1222.e3. https://doi.org/10.1016/j.neuron.2019.04.002

Joukal, M. (2017). Anatomy of the Human Visual Pathway. In K. Skorkovská (Ed.), Homonymous Visual Field Defects (pp. 1–16). Springer International Publishing. https://doi.org/10.1007/978-3-319-52284-5_1

Kaas, J. H., & Lyon, D. C. (2001). Chapter 18 Visual cortex organization in primates: Theories of V3 and adjoining visual areas. Progress in Brain Research, 134, 285–295. https://doi.org/10.1016/S0079-6123(01)34019-0

Kepecs, A., & Fishell, G. (2014). Interneuron cell types are fit to function. Nature, 505(7483), 318–326. https://doi.org/10.1038/nature12983

Kerschensteiner, D., & Guido, W. (2017). Organization of the dorsal lateral geniculate nucleus in the mouse. Visual Neuroscience, 34, E008. https://doi.org/10.1017/S0952523817000062

Kniestedt, C., & Stamper, R. (2003). Visual acuity and its measurement. Ophthalmology Clinics of North America, 16(2), 155–170. https://doi.org/10.1016/S0896-1549(03)00013-0

Knill, D. C., & Pouget, A. (2004). The Bayesian brain: The role of uncertainty in neural coding and computation. Trends in Neurosciences, 27(12), 712–719. https://doi.org/10.1016/j.tins.2004.10.007

Kok, P. (2015). Predictive Coding in Sensory Cortex. In E.-J. Wagenmakers & B. U. Forstmann (Eds.), An introduction to model-based cognitive neuroscience. Springer.

Kok, P., & de Lange, F. P. (2014). Shape Perception Simultaneously Up- and Downregulates Neural Activity in the Primary Visual Cortex. Current Biology, 24(13), 1531–1535. https://doi.org/10.1016/j.cub.2014.05.042

Kolb, B., & Whishaw, I. Q. (2015). Fundamentals of human neuropsychology (Seventh edition). Worth Publishers, a Macmillian Education Imprint.

Kolster, H., Peeters, R., & Orban, G., A. (2010). The Retinotopic Organization of the Human Middle Temporal Area MT/V5 and Its Cortical Neighbors. The Journal of Neuroscience, 30(29), 9801–9820. https://doi.org/10.1523/JNEUROSCI.2069-10.2010

Konen, C. S., & Kastner, S. (2008). Representation of Eye Movements and Stimulus Motion in Topographically Organized Areas of Human Posterior Parietal Cortex. Journal of Neuroscience, 28(33), 8361–8375. https://doi.org/10.1523/JNEUROSCI.1930-08.2008

Kubovy, M., Epstein, W., & Gepshtein, S. (2013). Visual Perception: Theoretical and Methodological Foundations. In I. B. Weiner, A. F. Healy, & R. W. Proctor (Eds.), Handbook of Psychology (2nd ed, Vol. 4, pp. 85–119). John Wiley & Sons.

Lawson, R. P., Bisby, J., Nord, C. L., Burgess, N., & Rees, G. (2021). The Computational, Pharmacological, and Physiological Determinants of Sensory Learning under Uncertainty. Current Biology, 31(1), 163-172.e4. https://doi.org/10.1016/j.cub.2020.10.043

Li, X., & Li, X. (2018). The Antidepressant Effect of Light Therapy from Retinal Projections. Neuroscience Bulletin, 34(2), 359–368. https://doi.org/10.1007/s12264-018-0210-1

Liem, F., Mérillat, S., Bezzola, L., Hirsiger, S., Philipp, M., Madhyastha, T., & Jäncke, L. (2015). Reliability and statistical power analysis of cortical and subcortical FreeSurfer metrics in a large sample of healthy elderly. NeuroImage, 108, 95–109. https://doi.org/10.1016/j.neuroimage.2014.12.035

Litwin, P., & Miłkowski, M. (2020). Unification by Fiat: Arrested Development of Predictive Processing. Cognitive Science, 44(7). https://doi.org/10.1111/cogs.12867

Lund, J. S., Boothe, R. G., & Lund, R. D. (1977). Development of neurons in the visual cortex (area 17) of the monkey (Macaca nemestrina): A Golgi study from fetal day 127 to postnatal maturity. The Journal of Comparative Neurology, 176(2), 149–187. https://doi.org/10.1002/cne.901760203

Markov, N. T., Vezoli, J., Chameau, P., Falchier, A., Quilodran, R., Huissoud, C., Lamy, C., Misery, P., Giroud, P., Ullman, S., Barone, P., Dehay, C., Knoblauch, K., & Kennedy, H. (2014). Anatomy of hierarchy: Feedforward and feedback pathways in macaque visual cortex. Journal of Comparative Neurology, 522(1), 225–259. https://doi.org/10.1002/cne.23458

McGilchrist, I. (2019). The Master and His Emissary: The Divided Brain and the Making of the Western World. https://www.degruyter.com/isbn/9780300247459

Meyer, T., & Olson, C. R. (2011). Statistical learning of visual transitions in monkey inferotemporal cortex. Proceedings of the National Academy of Sciences, 108(48), 19401–19406. https://doi.org/10.1073/pnas.1112895108

Milner, A. D. (2017). How do the two visual streams interact with each other? Experimental Brain Research, 235(5), 1297–1308. https://doi.org/10.1007/s00221-017-4917-4

Morgan, I. G., Wu, P.-C., Ostrin, L. A., Tideman, J. W. L., Yam, J. C., Lan, W., Baraas, R. C., He, X., Sankaridurg, P., Saw, S.-M., French, A. N., Rose, K. A., & Guggenheim, J. A. (2021). IMI Risk Factors for Myopia. Investigative Opthalmology & Visual Science, 62(5), 3. https://doi.org/10.1167/iovs.62.5.3

Morgan, J. L. (2017). A connectomic approach to the lateral geniculate nucleus. Visual Neuroscience, 34, E014. https://doi.org/10.1017/S0952523817000116

Muckli, L., Kohler, A., Kriegeskorte, N., & Singer, W. (2005). Primary Visual Cortex Activity along the Apparent-Motion Trace Reflects Illusory Perception. PLoS Biology, 3(8), e265. https://doi.org/10.1371/journal.pbio.0030265

Murray, S. O., Kersten, D., Olshausen, B. A., Schrater, P., & Woods, D. L. (2002). Shape perception reduces activity in human primary visual cortex. Proceedings of the National Academy of Sciences, 99(23), 15164–15169. https://doi.org/10.1073/pnas.192579399

Narr, K. L., Woods, R. P., Thompson, P. M., Szeszko, P., Robinson, D., Dimtcheva, T., Gurbani, M., Toga, A. W., & Bilder, R. M. (2007). Relationships between IQ and Regional Cortical Gray Matter Thickness in Healthy Adults. Cerebral Cortex, 17(9), 2163–2171. https://doi.org/10.1093/cercor/bhl125

Peyrache, A., Lacroix, M. M., Petersen, P. C., & Buzsáki, G. (2015). Internally organized mechanisms of the head direction sense. Nature Neuroscience, 18(4), 569–575. https://doi.org/10.1038/nn.3968

Pitcher, D., & Ungerleider, L. G. (2021). Evidence for a Third Visual Pathway Specialized for Social Perception. Trends in Cognitive Sciences, 25(2), 100–110. https://doi.org/10.1016/j.tics.2020.11.006

Poulere, E., Moschandreas, J., Kontadakis, G. A., Pallikaris, I. G., & Plainis, S. (2013). Effect of blur and subsequent adaptation on visual acuity using letter and Landolt C charts: Differences between emmetropes and myopes. Ophthalmic and Physiological Optics, 33(2), 130–137. https://doi.org/10.1111/opo.12020

Qiu, F. T., Sugihara, T., & von der Heydt, R. (2007). Figure-ground mechanisms provide structure for selective attention. Nature Neuroscience, 10(11), 1492–1499. https://doi.org/10.1038/nn1989

Qiu, F. T., & von der Heydt, R. (2005). Figure and Ground in the Visual Cortex: V2 Combines Stereoscopic Cues with Gestalt Rules. Neuron, 47(1), 155–166. https://doi.org/10.1016/j.neuron.2005.05.028

Reuter, M., Schmansky, N. J., Rosas, H. D., & Fischl, B. (2012). Within-subject template estimation for unbiased longitudinal image analysis. NeuroImage, 61(4), 1402–1418. https://doi.org/10.1016/j.neuroimage.2012.02.084

Rodríguez Martínez, G. A., & Castillo Parra, H. (2018). Bistable perception: Neural bases and usefulness in psychological research. International Journal of Psychological Research, 11(2), 63–76. https://doi.org/10.21500/20112084.3375

Romei, V., Driver, J., Schyns, P. G., & Thut, G. (2011). Rhythmic TMS over Parietal Cortex Links Distinct Brain Frequencies to Global versus Local Visual Processing. Current Biology, 21(4), 334–337. https://doi.org/10.1016/j.cub.2011.01.035

Rose, T., & Bonhoeffer, T. (2018). Experience-dependent plasticity in the lateral geniculate nucleus. Current Opinion in Neurobiology, 53, 22–28. https://doi.org/10.1016/j.conb.2018.04.016

Rossi, E. A., Weiser, P., Tarrant, J., & Roorda, A. (2007). Visual performance in emmetropia and low myopia after correction of high-order aberrations. Journal of Vision, 7(8), 14. https://doi.org/10.1167/7.8.14

RStudio, T. (2021). RStudio (1.2.5019) [Computer software]. RStudio: Integrated Development Environment for R. http://www.rstudio.com/

Ruff, C. C., Blankenburg, F., Bjoertomt, O., Bestmann, S., Weiskopf, N., & Driver, J. (2009). Hemispheric Differences in Frontal and Parietal Influences on Human Occipital Cortex: Direct Confirmation with Concurrent TMS–fMRI. Journal of Cognitive Neuroscience, 21(6), 1146–1161. https://doi.org/10.1162/jocn.2009.21097

Sabesan, R., & Yoon, G. (2010). Neural Compensation for Long-term Asymmetric Optical Blur to Improve Visual Performance in Keratoconic Eyes. Investigative Opthalmology & Visual Science, 51(7), 3835. https://doi.org/10.1167/iovs.09-4558

Schira, M. M., Tyler, C. W., Breakspear, M., & Spehar, B. (2009). The Foveal Confluence in Human Visual Cortex. Journal of Neuroscience, 29(28), 9050–9058. https://doi.org/10.1523/JNEUROSCI.1760-09.2009

Schmolesky, M. (1995). The Primary Visual Cortex. In H. Kolb, E. Fernandez, & R. Nelson (Eds.), Webvision: The Organization of the Retina and Visual System. University of Utah Health Sciences Center. http://www.ncbi.nlm.nih.gov/books/NBK11524/

Sereno, M. I., Dale, A. M., Reppas, J. B., Kwong, K. K., Belliveau, J. W., Brady, T. J., Rosen, B. R., & Tootell, R. B. H. (1995). Borders of Multiple Visual Areas in Humans Revealed by Functional Magnetic Resonance Imaging. Science, 268(5212), 889–893. https://doi.org/10.1126/science.7754376

Sereno, M. I., & Huang, R.-S. (2006). A human parietal face area contains aligned head-centered visual and tactile maps. Nature Neuroscience, 9(10), 1337–1343. https://doi.org/10.1038/nn1777

Shao, X., Guo, F., Shou, Q., Wang, K., Jann, K., Yan, L., Toga, A. W., Zhang, P., & Wang, D. J. J. (2021). Laminar perfusion imaging with zoomed arterial spin labeling at 7 Tesla. NeuroImage, 245, 118724. https://doi.org/10.1016/j.neuroimage.2021.118724

Shipp, S. (2016). Neural Elements for Predictive Coding. Frontiers in Psychology, 7. https://doi.org/10.3389/fpsyg.2016.01792

Sohoglu, E., & Chait, M. (2016). Detecting and representing predictable structure during auditory scene analysis. ELife, 5, e19113. https://doi.org/10.7554/eLife.19113

Spraul, C. W., & Lang, G. K. (2008). Optik und Refraktionsfehler. In Augenheilkunde (4., überarb. Aufl, pp. 314–339). Thieme.

Stachenfeld, K. L., Botvinick, M. M., & Gershman, S. J. (2017). The hippocampus as a predictive map. Nature Neuroscience, 20(11), 1643–1653. https://doi.org/10.1038/nn.4650

Stoeckel, C., Gough, P. M., Watkins, K. E., & Devlin, J. T. (2009). Supramarginal gyrus involvement in visual word recognition. Cortex, 45(9), 1091–1096. https://doi.org/10.1016/j.cortex.2008.12.004

Summerfield, C., & Egner, T. (2009). Expectation (and attention) visual cognition. Trends in Cognitive Sciences, 13(9), 403–409. https://doi.org/doi:10.1016/j.tics.2009.06.003

Summerfield, C., Trittschuh, E. H., Monti, J. M., Mesulam, M.-M., & Egner, T. (2008). Neural repetition suppression reflects fulfilled perceptual expectations. Nature Neuroscience, 11(9), 1004–1006. https://doi.org/10.1038/nn.2163

Thambisetty, M., Wan, J., Carass, A., An, Y., Prince, J. L., & Resnick, S. M. (2010). Longitudinal changes in cortical thickness associated with normal aging. NeuroImage, 52(4), 1215–1223. https://doi.org/10.1016/j.neuroimage.2010.04.258

Todorovic, A., & de Lange, F. P. (2012). Repetition Suppression and Expectation Suppression Are Dissociable in Time in Early Auditory Evoked Fields. Journal of Neuroscience, 32(39), 13389–13395. https://doi.org/10.1523/JNEUROSCI.2227-12.2012

Todorovic, A., van Ede, F., Maris, E., & de Lange, F. P. (2011). Prior Expectation Mediates Neural Adaptation to Repeated Sounds in the Auditory Cortex: An MEG Study. Journal of Neuroscience, 31(25), 9118–9123. https://doi.org/10.1523/JNEUROSCI.1425-11.2011

Tomczak, M., & Tomczak, E. (2014). The need to report effect size estimates revisited. An overview of some recommended measures of effect size. TRENDS in Sport Sciences, 1(21), 19–25.

Wagemans, J., Elder, J. H., Kubovy, M., Palmer, S. E., Peterson, M. A., Singh, M., & von der Heydt, R. (2012). A century of Gestalt psychology in visual perception: I. Perceptual grouping and figure–ground organization. Psychological Bulletin, 138(6), 1172–1217. https://doi.org/10.1037/a0029333

Wang, L., Mruczek, R. E. B., Arcaro, M. J., & Kastner, S. (2015). Probabilistic Maps of Visual Topography in Human Cortex. Cerebral Cortex, 25(10), 3911–3931. https://doi.org/10.1093/cercor/bhu277

Winawer, J., & Witthoft, N. (2015). Human V4 and ventral occipital retinotopic maps. Visual Neuroscience, 32, E020. https://doi.org/10.1017/S0952523815000176

Yantis, S., & Serences, J. T. (2003). Cortical mechanisms of space-based and object-based attentional control. Current Opinion in Neurobiology, 13(2), 187–193. https://doi.org/10.1016/S0959-4388(03)00033-3

Yon, D., & Frith, C. D. (2021). Precision and the Bayesian brain. Current Biology, 31(17), R1026–R1032. https://doi.org/10.1016/j.cub.2021.07.044

Zaretskaya, N. (2021). Zooming-in on higher-level vision: High-resolution fMRI for understanding visual perception and awareness. Progress in Neurobiology, 101998. https://doi.org/10.1016/j.pneurobio.2021.101998

Zaretskaya, N., Anstis, S., & Bartels, A. (2013). Parietal Cortex Mediates Conscious Perception of Illusory Gestalt. Journal of Neuroscience, 33(2), 523–531. https://doi.org/10.1523/JNEUROSCI.2905-12.2013